



Future projection of Indian summer monsoon variability under climate change scenario: An assessment from CMIP5 climate models



S. Sharmila, S. Joseph, A.K. Sahai *, S. Abhilash, R. Chattopadhyay

Indian Institute of Tropical Meteorology, Pune-411008, India

ARTICLE INFO

Article history:

Received 9 May 2014

Received in revised form 18 October 2014

Accepted 14 November 2014

Available online 20 November 2014

Keywords:

monsoon variability

climate change

future projection

CMIP5

ABSTRACT

In this study, the impact of enhanced anthropogenic greenhouse gas emissions on the possible future changes in different aspects of daily-to-interannual variability of Indian summer monsoon (ISM) is systematically assessed using 20 coupled models participated in the Coupled Model Inter-comparison Project Phase 5. The historical (1951–1999) and future (2051–2099) simulations under the strongest Representative Concentration Pathway have been analyzed for this purpose. A few reliable models are selected based on their competence in simulating the basic features of present-climate ISM variability. The robust and consistent projections across the selected models suggest substantial changes in the ISM variability by the end of 21st century indicating strong sensitivity of ISM to global warming. On the seasonal scale, the all-India summer monsoon mean rainfall is likely to increase moderately in future, primarily governed by enhanced thermodynamic conditions due to atmospheric warming, but slightly offset by weakened large scale monsoon circulation. It is projected that the rainfall magnitude will increase over core monsoon zone in future climate, along with lengthening of the season due to late withdrawal. On interannual timescales, it is speculated that severity and frequency of both strong monsoon (SM) and weak monsoon (WM) might increase noticeably in future climate. Substantial changes in the daily variability of ISM are also projected, which are largely associated with the increase in heavy rainfall events and decrease in both low rain-rate and number of wet days during future monsoon. On the subseasonal scale, the model projections depict considerable amplification of higher frequency (below 30 day mode) components; although the dominant northward propagating 30–70 day mode of monsoon intraseasonal oscillations may not change appreciably in a warmer climate. It is speculated that the enhanced high frequency mode of monsoon ISOs due to increased GHG induced warming may notably modulate the ISM rainfall in future climate. Both extreme wet and dry episodes are likely to intensify and regionally extend in future climate with enhanced propensity of short active and long break spells. The SM (WM) could also be more wet (dry) in future due to the increment in longer active (break) spells. However, future changes in the spatial pattern during active/break phase of SM and WM are geographically inconsistent among the models. The results point out the growing climate-related vulnerability over Indian subcontinent, and further suggest the requisite of profound adaptation measures and better policy making in future.

© 2014 Elsevier B.V. All rights reserved.

1. Introduction

The global warming due to the gradual increase in the anthropogenic greenhouse gas (GHG) emissions is unequivocal (IPCC, 2007). Multi-model projections of future global monsoon indicate significant increase in the monsoon area and precipitation in GHG-induced warmer climate (Hsu et al., 2012; Kitoh et al., 2013; Lau et al., 2013; Lee and Wang, 2014), leading to more severe hydro-climatic extremes like floods, droughts and extreme events in future. However, the response of different regional monsoons to changing climate may vary due to distinctive

land-ocean configuration, orography and forcing (Cherchi et al., 2011; Turner and Annamalai, 2012). Nevertheless, the future projections of regional monsoons still remain largely uncertain (IPCC, 2007) and need more careful investigations.

The Indian summer monsoon (ISM) is one of the most energetic and vigorous regional monsoon systems and exhibits highly complex spatio-temporal variability during June-September (JJAS) (Goswami, 2011). As the monsoon has strong sensitivity to global warming (Kitoh et al., 2013), it is expected that the unprecedented enhancement of GHG emissions in the recent times could rather aggravate the complexity and severity of ISM. Such potential consequences could amplify the extreme behaviour of ISM leading to disastrous impacts on the agricultural production, ecosystems, health and food security, agrarian-based economy over this subcontinent (e.g. Gadgil and Rupa Kumar, 2006). The realistic projections on future behaviour of ISM variability

* Corresponding author.

E-mail addresses: sharmila@tropmet.res.in (S. Sharmila), susmitha@tropmet.res.in (S. Joseph), sahai@tropmet.res.in (A.K. Sahai), abhi@tropmet.res.in (S. Abhilash), rajib@tropmet.res.in (R. Chattopadhyay).

are thus imperative for making sustainable economic development and better future adaptation measurements over largely populated Indian subcontinent.

Investigations involving the emerging effects of atmospheric warming on changing the dynamics and thermodynamics of ISM have already been started since late-twentieth century. Some observational studies show significant increase in the frequency of extreme precipitation events (Goswami et al., 2006; Rajeevan et al., 2008) and declining trend in low-to-moderate rainfall events and low level circulation associated with ISM over Indian subcontinent since 1950's (Dash et al., 2009). On contrary, the analysis of 131 years (1871–2001) observational data could not find any clear evidence of changes in ISM strength and its interannual variability (IAV) (Kripalani et al., 2003; Guhathakurta and Rajeevan, 2008). Recently, Ghosh et al. (2012) also found lack of uniform trends during the period of (1951–2003), but an increase in the spatial variability of observed rainfall extremes. However, in contrast, recent study by Singh et al. (2014) demonstrated statistically significant changes in the extreme wet and dry spells in the recent decades by analyzing between two periods of the observed record (1951–1980) and (1981–2011). Hence, extensive debates still exist in understanding the possible modulation of the observed space-time characteristics of ISM variability and its provenance to climate change.

Climate models could be useful tools to simulate present climate and can provide quantitative estimates of the future climate variability. Over the last two decades, several modelling studies have been attempted to address this issue using different sensitivity experiments. On the seasonal scale, most of these studies suggested intensification of ISM rainfall in future warmer climate due to the anticipated increase in GHG concentrations (Meehl and Wahsington, 1993; Hu et al., 2000; May, 2004, 2011; Kripalani et al., 2007; Turner et al., 2007; Stowasser et al., 2009; Cherchi et al., 2011; Krishna Kumar et al., 2011). Despite future increase in monsoon rainfall, many studies are also suggestive of the weakening of both the cross-equatorial monsoon flow and tropical large scale overturning circulations in response to anthropogenic forcing (Kitoh et al., 1997; Tanaka et al., 2005; Ueda et al., 2006; Stowasser et al., 2009; Krishnan et al., 2013), which is popularly known as the precipitation-wind paradox (Ueda et al., 2006). Most of these modelling studies advocate the role of increased preferable thermodynamic conditions over ISM region for the intensification of monsoon rainfall leading to the 'wet-get-wetter' situation (Held and Soden, 2006) in response to greenhouse warming (Bhaskaran et al., 1995; Kitoh et al., 1997; Hu et al., 2000; Lal et al., 2001; May, 2004, 2011; Rupa Kumar et al., 2006; Turner et al., 2007; Cherchi et al., 2011). The combination of warmer Indian Ocean and enhanced low-level moisture convergence have been found to play significant role in increasing monsoon rainfall despite the weakened south-westerly monsoon flow through reduction in meridional thermal gradient (Dairaku and Emori, 2006; Ueda et al., 2006; Meehl et al., 2007; Stowasser et al., 2009; Turner, 2011). In contrast, few other studies found drier monsoon due to the dominant future dynamical feedback in a warmer climate (Ashfaq et al., 2009; Annamalai et al., 2013). Some of the above studies also projected increase in IAV of monsoon rainfall in future climate (e.g. Hu et al., 2000; May, 2004; Turner et al., 2007), while Turner et al. (2007) found increased coupling between modelled IAV of monsoon rainfall and wind strength under future emission scenario, which appears highly uncertain. In addition, no clear suggestions have been made on the seasonal projection of future frequency and spatial changes in the extremes IAV of ISM; namely strong monsoon (SM) and weak monsoon (WM) seasons (Annamalai, 2011). The presence of such uncertainties and lack of robustness among the models contribute to the large spread in the future ISM projection. Therefore, the projection of ISM on seasonal to interannual timescale still remains highly uncertain and regionally variable under warmer climate (IPCC, 2007; Krishna Kumar et al., 2011).

On the other hand, very few studies have assessed the future projections of the monsoon intraseasonal variability (ISV). Within the ISM

variability, the dominant intraseasonal (10–90 day mode) quasi-periodic monsoon intraseasonal oscillations (ISOs) are considered as the major building blocks of the ISM rainfall as they manifest in the form of active/break episodes over Indian subcontinent (Goswami, 2011). The duration and frequency of these wet/dry spells within a monsoon season contributes to the seasonal mean rainfall, and thus modulates the IAV of ISM (Goswami, 2011); e.g. prolonged actives/breaks during critical crop growth period severely damage the agricultural yields, and any possible change in response to GHG warming will cause cascading impacts on socio-economic condition over India. Therefore, it is necessary to understand the possible response of monsoon ISOs and associated active-break cycles to the GHG warming. Based on the Coupled Model Intercomparison Project Phase 3 (CMIP3) multi-model dataset, Mandke et al. (2007) analyzed the sensitivity of active-break cycles in response to GHG forcing and found the break spells to intensify and extend in the future, however there were inconsistency among different scenarios of the same models. Turner and Slingo (2009) further noted an intensification of both active and break events relative to seasonal cycle, without any suggestion on any change to the duration or likelihood of monsoon breaks. However, precise assessments of such regional projections based on CMIP3 multi-models have remained highly uncertain due to variations among the model projections as well as the models' limited ability to simulate ISV of ISM.

Recently, the multi-model data archive of CMIP Phase 5 (CMIP5; Taylor et al., 2012) has been released in preparation of the Intergovernmental Panel on Climate change (IPCC) fifth assessment report (IPCC-AR5) under which a series of experiments including the 20th century historical simulation and 21st century climate projections with four different representative concentration pathway (RCP) were performed using various coupled general circulation models (CGCMs) developed by a number of international climate modelling groups from around the world. Compared to CMIP3, the CMIP5 models are better in terms of representing model physics, resolutions, inclusion of atmospheric aerosols (Sperber et al., 2012; Taylor et al., 2012). Even some models are Earth System Models (ESMs) that include the changes in the earth climate system. The CMIP5 models are found to be far better than CMIP3 in representing Asian-Australian monsoon matrices (Wang et al., 2014). In addition, CMIP5 models project a larger increase in annual mean precipitation over the entire Asian monsoon region with less uncertainty than CMIP3 (Lee and Wang, 2014). Therefore, the CMIP5 models can be utilised for better projection of the future ISM variability. Recent studies have already investigated the overall future changes in global monsoon precipitation using multi-model ensemble and/or selected CMIP5 models under different range of RCP scenarios (Hsu et al., 2012, 2013; Wang et al., 2014; Kitoh et al., 2013; Lee and Wang, 2014), that suggest notable increase in global monsoon precipitation during 21st century due to global warming. However, by comparing the future projections between RCP4.5 (moderate) and RCP8.5 (strongest) scenarios, Kitoh et al. (2013) suggested that the global monsoon response to atmospheric warming is larger and more robust in a warmer RCP8.5 world among the models. Motivated by these key issues, the present study utilizes the historical simulations of (1951–1999) and future projections of (2051–2099) under the strongest RCP8.5 scenario in an attempt to demonstrate a more robust future projection of ISM variability (from daily to sub-seasonal, and seasonal to interannual time scales) based on standard and careful diagnosis. Therefore, the main objectives of this study are: to evaluate the fidelity of around 20 CMIP5 models in simulating the basic features of ISM variability of the present climate and selection of most reliable models to investigate the potential future changes in ISM variability under the strongest RCP8.5 scenario emphasizing the emerging role of increased anthropogenic GHGs emissions in changing the future ISM.

The paper is organized as follows: The models, data and method used in the present study are described in Section 2. The future projections of ISM variability from CMIP5 models are discussed in Sections 3 and 4 summarizes the important conclusions of this paper.

2. Model, data and methodology

2.1. CMIP5 models and experiments

To assess the future change in ISM under climate change scenario, the simulations from historical (1951–1999) and RCP8.5 (2051–2099) experiments are analyzed. The historical runs (20th century simulations) are forced by observed transient climate forcings from the instrumental period (solar, volcanoes, GHGs concentrations, reconstructed aerosol emission etc). Initial conditions are based on a long equilibrium control run with fixed pre-industrial forcings. The RCP8.5 runs (21st century simulations) are forced with relatively high anthropogenic GHGs emissions, designed so that anthropogenic radiative forcing will increase and then stabilize at about 8.5Wm^{-2} after 2100. Initial conditions for the RCP8.5 scenario start from the end of the historical runs. Similar future projections under RCP4.5 scenario are also used for comparison. In this study, outputs from 20 CMIP5 models (Table 1) including daily precipitation, the zonal, meridional wind, vertical pressure velocity, temperature and specific humidity at all available levels of both experiments are used for analysis. For each model, only one ensemble member (r1i1p1) run has been used (similar to Kitoh et al., 2013). More details on models and experiments can be found in Taylor et al. (2012). All model outputs are freely accessible at <http://pcmdi9.llnl.gov/esgf-web-fe/> maintained by Earth System Grid Federation (ESGF).

2.2. Datasets used

To validate the CGCMs in their historical simulations with respect to observations in terms of daily precipitation, observed high resolution daily gridded rainfall data over Indian land region from National Climate Centre (NCC), India Meteorological Department (IMD), Pune (Rajeevan et al., 2006), and satellite based daily Global Precipitation Climatology Project (GPCP) precipitation data (Huffman et al., 2009) are used. The reanalysis data of daily circulation from National Centers for Environmental Prediction/National Center for Atmospheric Research (NCEP/NCAR; Kalnay et al., 1996) are also used for calculating long-term dynamical monsoon indices.

2.3. Methodology

All model outputs are interpolated into common $2.5^\circ \times 2.5^\circ$ grid by bilinear interpolation. The overall fidelity of each model to simulate seasonal mean ISM and its variability of the present climate is assessed using Taylor diagram metric (Taylor, 2001). Taylor diagrams are well accepted performance metrics for climate models that provide a brief statistical outline of how well spatial/temporal patterns match each other in terms of their correlation coefficients (CC), their root-mean-square error (RMSE), and the simulated to observed ratio of their variances. The distance from the origin indicates the normalized standard deviation (NSD) of each model. Using this metric, the model having the largest CC, normalized standard deviation close to the unity (i.e.; close to the observation) and smaller RMSE is considered to be the best among them.

The IAV of ISM strength is analyzed using multiple summer monsoon indices. The all-India Rainfall (AIR) index (from JJAS rainfall area-averaged over Indian land points) and different dynamical monsoon indices (DMIs) are computed for all selected models to make projection on the future association between rainfall and wind strength on interannual time scales. The three DMIs related to wind shear have been used: (1) vertical shear of zonal wind (WY Index; Webster and Yang, 1992), (2) horizontal shear of zonal wind (WF Index; Wang and Fan, 1999) and (3) vertical shear of meridional wind (MH Index; Goswami et al., 1999). Further, the extremes of IAV; i.e. SM and WM years are identified when AIR $\geq +1.0$ and ≤ -1.0 respectively.

The daily anomalies are computed by subtracting daily smoothed (mean + 1st three harmonics) long term climatology for all the datasets. To understand the space-time behaviour of monsoon ISOs, limited domain meridional wavenumber frequency spectra analysis (following Wheeler and Kiladis, 1999; Joseph et al., 2012) is performed on daily precipitation during May to October over ISM region. To extract dominant ISV of ISM, Lanczos filter (Duchon, 1979) has been applied on daily anomalies. An extended empirical orthogonal function (EOF) analysis is also performed on intraseasonally filtered daily precipitation over ISM domain (15°S – 30°N and 65° – 95°E) during June to September to extract the monsoon ISO evolution. The 30–70 day filtered daily

Table 1

List of CMIP5 models selected for this study along with modelling groups and the horizontal/vertical resolution of the corresponding atmosphere/ocean models.

| CMIP5 model | Modelling group | AGCM resolu. | OGCM resolu. |
|----------------|--|-------------------------------------|----------------------------|
| ACCESS1.0 | Commonwealth Scientific and Industrial Research Organization (CSIRO) and Bureau of Meteorology, (BOM), Australia | $1.25^\circ \times 1.875^\circ$ L38 | |
| ACCESS1.3 | Commonwealth Scientific and Industrial Research Organization (CSIRO) and Bureau of Meteorology, (BOM), Australia | $1.25^\circ \times 1.875^\circ$ L38 | |
| BCC-CSM1.1 | Beijing Climate Centre, China Meteorological Administration, China | T42L26 | 1×1.33 L40 |
| BNU-ESM | College of Global Change and Earth System Science, Beijing Normal University, China | T42L26 | |
| CanESM2 | Canadian Centre for Climate Modelling and Analysis, Canada | T63L35 | 256×192 L40 |
| CSIRO-Mk3.6.0 | Commonwealth Scientific and Industrial Research Organization in collaboration with the Queensland Climate Change Centre of Excellence, Australia | T63L18 | 1.875×-0.9375 L31 |
| GFDL-CM3 | Geophysical Fluid Dynamics Laboratory, USA | $2^\circ \times 2.5^\circ$ L48 | 360×200 L50 |
| GFDL-ESM2G | Geophysical Fluid Dynamics Laboratory, USA | $2^\circ \times 2.5^\circ$ L24 | 360×210 L63 |
| GFDL-ESM2M | Geophysical Fluid Dynamics Laboratory, USA | $2^\circ \times 2.5^\circ$ L24 | 360×200 L50 |
| HadGEM2-ES | Met Office Hadley Centre, UK | $1.25^\circ \times 1.875^\circ$ L38 | 1×0.3 – 1.0 L40 |
| INMCM4 | Institute for Numerical Mathematics, Russia | $1.5^\circ \times 2.0^\circ$ L21 | 1×0.5 L40 |
| IPSL-CM5A-LR | Institut Pierre-Simon Laplace, France | $1.875^\circ \times 3.75^\circ$ L39 | 2×2 L31 |
| IPSL-CM5A-MR | Institut Pierre-Simon Laplace, France | $1.25^\circ \times 2.5^\circ$ L39 | 2×2 L31 |
| IPSL-CM5B-LR | Institut Pierre-Simon Laplace, France | $1.875^\circ \times 3.75^\circ$ L39 | |
| MIROC5 | Atmosphere and Ocean Research Institute (The University of Tokyo), National Institute for Environmental Studies, and Japan Agency for Marine-Earth Science and Technology | T85L40 | 256×224 L50 |
| MIROC-ESM-CHEM | Japan Agency for Marine-Earth Science and Technology, Atmosphere and Ocean Research Institute (The University of Tokyo), and National Institute for Environmental Studies, Japan | T42L80 | 256×192 L44 |
| MPI-ESM-LR | Max Planck Institute for Meteorology (MPI-M), Germany | T63L47 | |
| MPI-ESM-MR | Max Planck Institute for Meteorology (MPI-M), Germany | T63L95 | GR15 L40 |
| MRI-CGCM3 | Meteorological Research Institute, Japan | T159L48 | 256×192 L44 |
| NorESM1-M | Norwegian Climate Centre, Norway | $1.875^\circ \times 2.5^\circ$ | 384×320 L53 |

precipitation is then lag-regressed onto first EEOF mode to capture the dominant northward propagating monsoon ISOs for all the simulations. In addition, to identify the active-break cycles associated with monsoon ISV, a rainfall index (RI) is computed by applying a 10–90 day band-pass filter to the daily rainfall anomalies area-averaged over core monsoon zone (similar to Rajeevan et al., 2010) for each year normalized by its own standard deviation. The active (break) spells are identified

such that $RI >= +1.0$ (≤ -1.0) for at least consecutive 3 days or more for all the years. The Identification procedure is done from 15 June to 20 September of each year.

Further, the daily equivalent potential temperature (θ_e), atmospheric dry static stability, moisture convergence flux are also computed for both simulations to investigate the change in thermodynamic conditions in response to enhanced GHG induced warming.

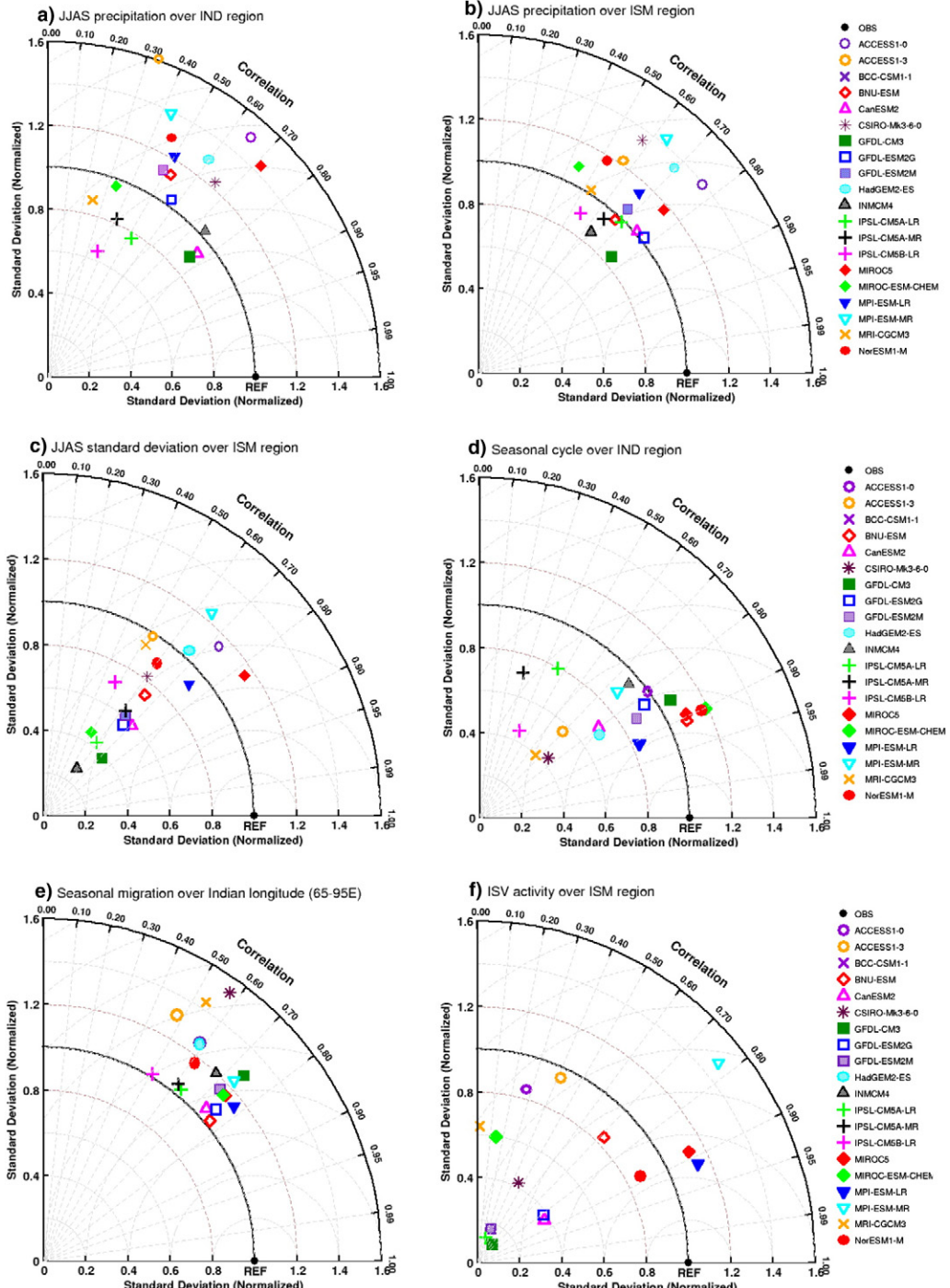


Fig. 1. Selection of better CMIP5 models using Taylor diagrams: a) climatological seasonal mean (JJAS) precipitation over IND region (Indian land points only), b) JJAS mean precipitation over Indian monsoon region [15°S – 30°N ; 50° – 120°E], c) JJAS standard deviation of precipitation over Indian subcontinent, d) mean seasonal cycle (May to October) over IND region, e) mean seasonal migration of precipitation over Indian longitude [65° – 95°E], and f) mean ISV variance of 10–90 day filtered daily precipitation anomalies over Indian monsoon region [15°S – 30°N ; 50° – 120°E] during JJAS as simulated by 20 models and their comparison with observation.

Table 2

Model performance criteria used to select better CMIP5 models in simulating basic characteristics of Indian summer monsoon for this study. Selected models are highlighted in bold.

| CMIP5 models | Rainfall simulation (Historical) Criteria : CC≥0.5 and 0.8≤NSD≤1.2 | | | | | | Total (out of 6) |
|-------------------|--|---------------|------------------|-------------------|-----------------------|--------------|---------------------|
| | JJAS (IND) | JJAS (ISM) | JJAS std dev. | Seasonal cycle | Seasonal migration | ISO variance | |
| ACCESS1-0 | – | – | + | + | – | – | 2 |
| ACCESS1-3 | – | – | + | – | – | – | 1 |
| BCC-CSM1-1 | – | – | – | – | – | – | 0 |
| BNU-ESM | + | + | – | + | + | + | 5 |
| CanESM2 | + | + | – | – | + | – | 3 |
| CSIRO-Mk3-6-0 | – | – | + | – | – | – | 1 |
| GFDL-CM3 | + | + | – | + | – | – | 3 |
| GFDL-ESM2G | + | + | – | + | + | – | 4 |
| GFDL-ESM2M | – | + | – | + | + | – | 3 |
| HadGEM2 | – | – | + | – | – | – | 1 |
| INMCM4 | + | + | – | + | + | – | 4 |
| IPSL-CM5A-LR | – | + | – | – | + | – | 2 |
| IPSL-CM5A-MR | – | + | – | – | + | – | 2 |
| IPSL-CM5B-LR | – | + | – | – | + | – | 2 |
| MIROC5 | – | + | + | + | + | + | 5 |
| MIROC-ESM-CHEM | – | – | – | + | + | – | 2 |
| MPI-ESM-LR | – | + | + | + | + | + | 5 |
| MPI-ESM-MR | – | + | – | + | – | – | 2 |
| MRI-CGCM3 | – | – | – | + | – | – | 1 |
| NorESM1-M | – | + | + | + | + | + | 5 |

3. Results and discussions

3.1. Model selection

Before projecting the possible future changes, it is essential to evaluate the fidelity of these CMIP5 CGCMs in simulating observed ISM and its variability. All 20 CGCMs may not represent ISM realistically and hence their projection will be more or less uncertain. Hence, instead of creating a multi-model ensemble of all available CMIP5 models, the usage of better climate models in terms of their performance in simulating realistic ISM variability would be beneficial for making reliable projections. Therefore, a set of six performance metrics has been employed in choosing better models compared to observations (OBS hereafter). The evaluation metrics includes spatial/temporal patterns of (1) climatological seasonal (JJAS) mean precipitation over Indian land points [IND region], (2) JJAS mean precipitation over Indian summer monsoon region [15°S – 30°N ; 50° – 120°E , ISM region], (3) JJAS standard deviation of precipitation over extended IND region, (4) mean seasonal cycle over IND region, (5) mean seasonal migration of daily precipitation over Indian longitude [65° – 95°E] and (6) the intraseasonal (10–90-day

filtered) variance of June–September daily precipitation over ISM region using Taylor diagrams (Fig. 1; method briefly discussed in Section 2.3).

We define the criteria for the performance metrics as models having at least $\text{CC} \geq 0.5$ and $0.8 \leq \text{NSD} \leq 1.2$ in simulating most of the above features of ISM and its variability. From Fig. 1a, it seems that simulating the spatial pattern of JJAS precipitation perfectly over IND region compared to IMD rainfall is still a difficult task for most of the models. Only GFDL-CM3, CanESM2, INMCM4, GFDL-ESM2G are able to reproduce it to some extent. However, over ISM region many models could capture the observed spatial patterns having $\text{CC} > 0.65$ (Fig. 1b). Taylor diagram of the JJAS standard deviation of precipitation (Fig. 1c) shows that MIROC5, MPI-ESM-LR, HadGEM2-ES, ACCESS1-0, NorESM1-M perform better than others, while in simulating May to October seasonal cycle of daily precipitation (Fig. 1d), mainly ACCESS1-0, BNU-ESM, MIROC5, MIROC-ESM-CHEM, MPI-ESM-LR, MPI-ESM-MR, NorESM1-M and all GFDL models perform well. Fig. 1e shows that most of the models (except ACCESS1-3, BCC-CSM1-1, CSIRO-Mk3-6-0, HadGEM2-ES, MRI-CGCM3) simulate the seasonal migration of daily rainfall over Indian region reasonably. However, most importantly, only BNU-ESM, MPI-ESM-LR, MIROC5 and NorESM1-M could simulate the spatial

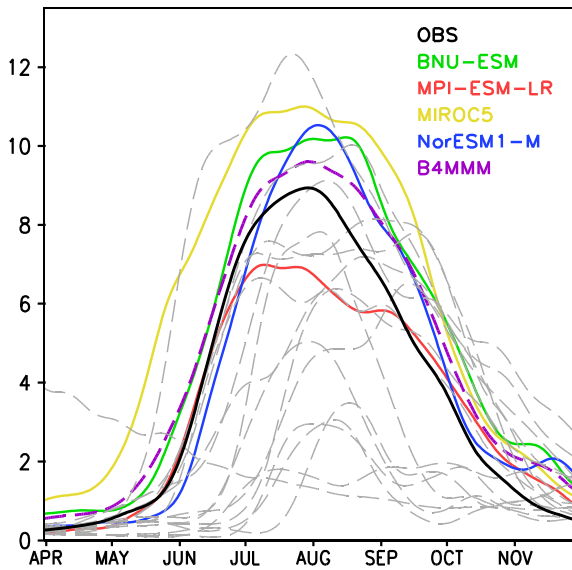


Fig. 2. Seasonal cycle of daily precipitation over Indian land region from observation (IMD; Black) and 20 CMIP5 model simulations (historical). The selected models and their MMM are shown in colour.

pattern of intraseasonal variance over ISM region reasonably compared to GPCP (Fig. 1f). Therefore, based on our model performance criteria, only 4 models (BNU-ESM, MPI-ESM-LR, MIROC5 and NorESM1-M) are found to be better among all 20 models in simulating ISM and its variability (Table 2).

Interestingly 3 out 4 models are the ESMs, therefore, providing more promise over other CGCMs. Recent studies also show that NorESM1-M and MIROC5 have the largest skill score in simulating mean state of global as well as Asian-Australian monsoon (Lee and Wang, 2014; Wang et al., 2014), and MPI-ESM-LR have large skill score on intraseasonal timescales (Sperber et al., 2012). Sabeerali et al. (2013)

noted that BNU-ESM, MIROC5, and MPI-ESM-LR are better in simulating realistic boreal summer ISOs variance over extended monsoon region. Fig. 2 shows the simulated present climate evolution of the seasonal cycle of daily precipitation over IND region, where only the best 4 models and their mean (B4MMM hereafter) are shown in colour with respect to observation (black). Although MIROC5 (MPI-ESM-LR) slightly overestimates (underestimates) the rainfall magnitude possibly due to wet (dry) bias over central Indian region, it is noted that all best 4 models together with B4MMM reproduce the present-climate seasonal cycle quite realistically relative to OBS. In the following subsections, the projections of ISM variability using these models are shown systematically.

3.2. Projected changes in seasonal mean state of ISM

The projected seasonal cycle of daily precipitation over central Indian region under moderate RCP4.5 (dash blue curve) and strongest RCP8.5 scenarios (solid red curve) with respect to present climate (green curve), along with their changes are initially assessed and shown in Fig. 3. Substantial potential increase in the rainfall maxima and length of summer monsoon season are projected in changing climate under both the scenarios (Fig. 3a). Further, B4MMM suggests that rainfall magnitude is likely to increase in future and the duration of the rainy season may also lengthen due to delayed withdrawal, although not much changes in monsoon onset is expected (Fig. 3a). Fig. 3b further demonstrates that the likelihood of future changes in both magnitude and evolution is more robust and consistent among the selected models under RCP8.5 scenario compared to RCP4.5 as suggested by previous studies (Kitoh et al., 2013). Hence, the present study further assesses the future changes in ISM variability under the RCP8.5 scenario only.

The projected relative changes in the spatial pattern of seasonal mean rainfall over ISM region are shown in Fig. 4a–e. Model projections indicate that the JJAS mean precipitation will enhance about 10–25% over Indian subcontinent (Fig. 4a–e) relative to present climate. However, MPI-ESM-LR shows a decreased rainfall over north-west Indian

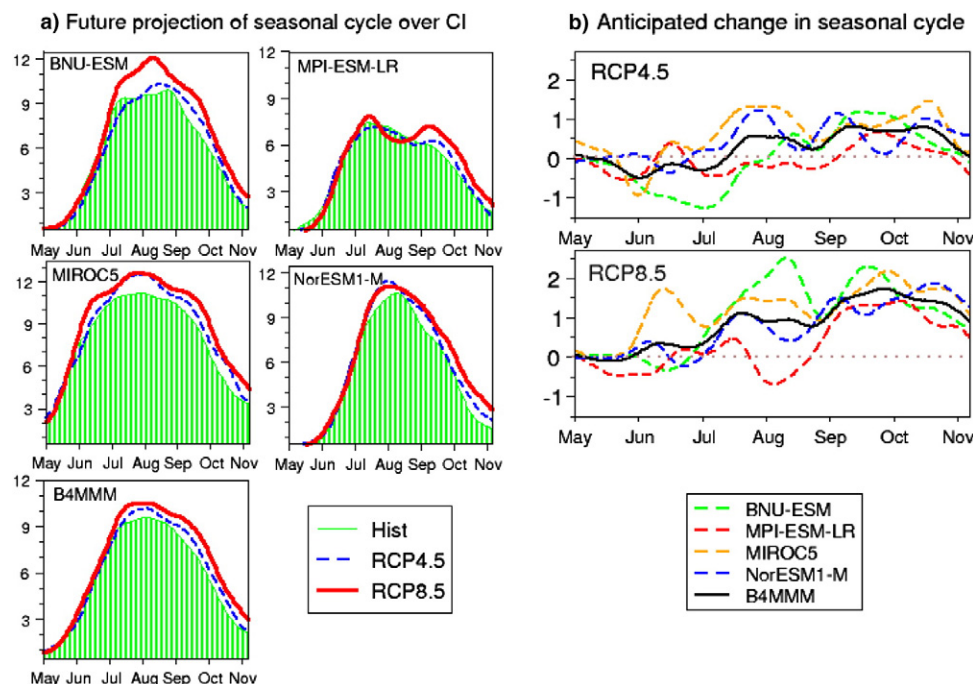


Fig. 3. (a) Present climate (historical; green curve) and projected future changes in mean seasonal cycle of daily precipitation over central Indian region (CI) under RCP4.5 (blue; dash) and RCP8.5 (red; solid) scenarios for selected CMIP5 models and their MMM. The anticipated changes in seasonal cycles under these scenarios are shown in (b).

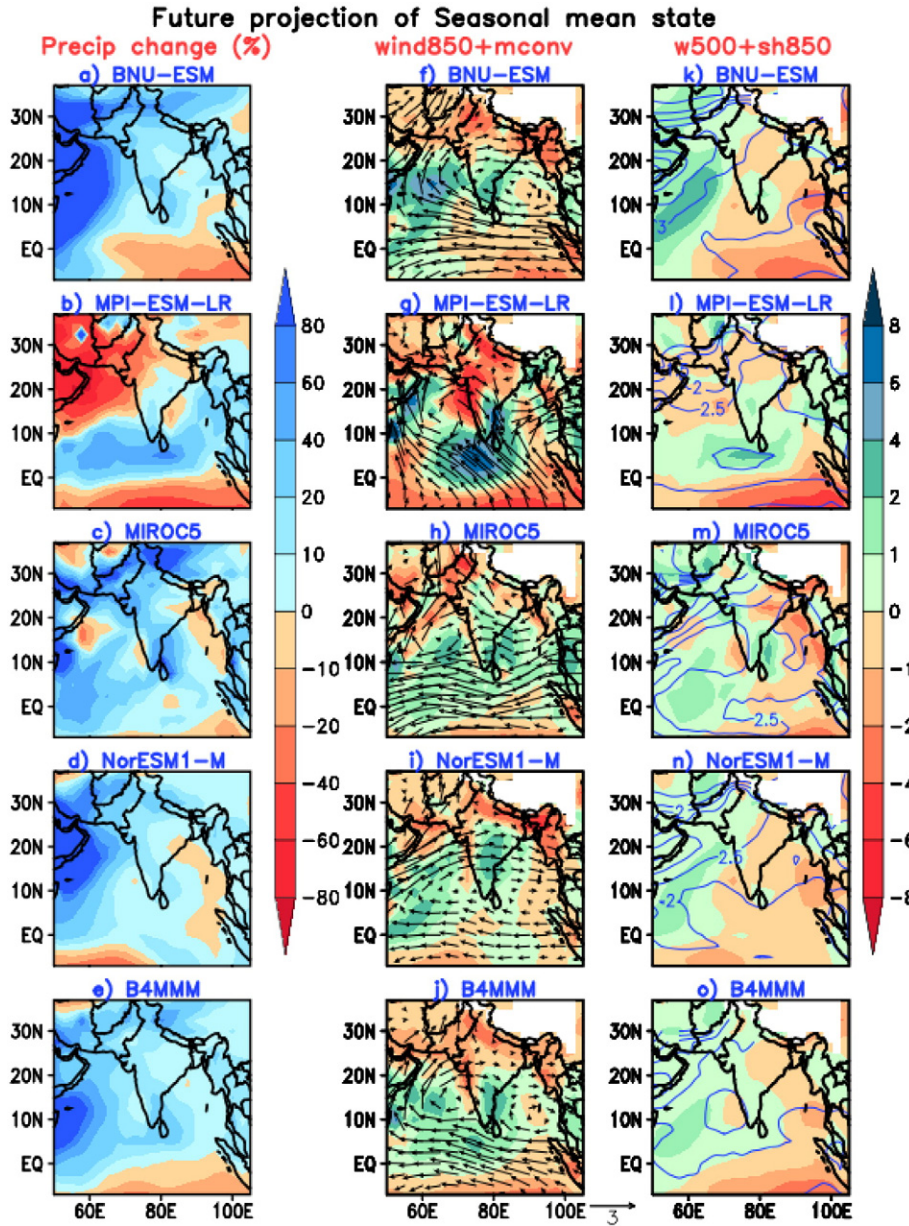


Fig. 4. Projected spatial changes in the seasonal mean state of ISM under RCP8.5 scenario: Relative changes^a (%) in JJAS rainfall are shown in a–e, changes (RCP8.5 –Hist) to the low level circulation (850 hPa; vector) and vertically integrated (surface to 500 hPa) moisture convergence flux (shaded) are shown in f–j, and changes to omega (at 500 hPa; shaded; positive values represents ascending motion) and specific humidity (at 850 hPa; contour) are shown in k–o for the selected CMIP5 models and their MMM. The changes are calculated between the period 2051–2099 and 1951–1999.^a ($X_{\text{RCP8.5}} - X_{\text{Hist}}$) / X_{Hist} .

region and adjoining northern Arabian Sea. The B4MMM projects overall increased rainfall over central-west to peninsular Indian region as well as most part of ISM region; but rainfall increase over the eastern region is not very remarkable. In addition, a slight decrease over head Bay of Bengal and substantial suppression of rainfall over the east equatorial Indian Ocean (EEIO) are also projected. It is noteworthy that a north-south asymmetry in the JJAS mean rainfall over ISM region is evident in the models. To understand the projected dynamical and thermodynamical feedbacks associated with the rainfall change, the change in seasonal mean low-level circulation (vector) overlaid with vertically integrated (surface to 500 hPa) moisture convergence flux (shaded) are presented in Fig. 4f–j. In addition, the JJAS change in vertical pressure velocity (omega) at 500 hPa (shaded) overlaid with specific humidity at 850 hPa (contour) is also shown in Fig. 4k–o for selected models. The B4MMM shows that the general increase in ISM rainfall may be primarily driven by the intensified low level moisture convergence (Fig. 4j)

due to considerable enhancement of atmospheric moisture content (Fig. 4o) over ISM region in response to increased GHG warming. However, local change in moisture convergence varies geographically over Indian subcontinent; e.g. it is projected that the moisture convergence

Table 3

Simulated mean all-India summer monsoon rainfall (ISM) and interannual standard deviation (SD) and corresponding projected change under RCP8.5 scenario for selected models.

| Model | Historical (1951–1999) | | RCP8.5 (2051–2099) | |
|------------|------------------------|--------------|--------------------|--------------|
| | Mean | SD | Mean | SD |
| Observed | 856.14 | 85.35 | - | - |
| BNU-ESM | 810.73 | 70.86 | 938.54 | 82.85 |
| MPI-ESM-LR | 642.33 | 59.86 | 656.69 | 78.68 |
| MIROC5 | 1013.24 | 85.82 | 1149.04 | 82.23 |
| NorESM1-M | 882.60 | 89.03 | 971.85 | 91.73 |
| B4MMM | 837.23 | 76.39 | 929.03 | 83.87 |

will be reduced over the regions of least intense rainfall, i.e.; northwest India and north-east India. This may be related to the difference in the dynamical feedback change over ISM region in future climate. Projections on low level monsoon circulation changes show weakening of the cross-equatorial westerlies (Fig. 4j) over Arabian Sea with the northward shift of the moisture flux. The large decrease of rainfall over EEIO may be related to the projected strong subsidence from the enhanced convection over warmer Western Pacific connected through an overturning circulation (Fig. 4e and Fig. 4o). A pair of anticyclones in the lower level (one over the Bay of Bengal and another over 10°S of EIO) are projected as Rossby wave response to the largely decreased rainfall over EEIO. These projected circulation change along with westward shift of extended anticyclonic circulation from North-Western Pacific may strengthen the easterly anomaly along the EIO, resulting in the weakening of the cross equatorial seasonal mean low level circulation, consistent with previous studies (Stowasser et al., 2009; May, 2011). Also an anomalous anticyclonic circulation is collocated around 10–15°N (Fig. 4j) along with low level humidity maxima near the west coast of Indian subcontinent over warmer Indian Ocean (Fig. 4o). Such changes in local circulation may enhance local evaporation that favours the intensification of JJAS mean rainfall over these regions. It is noted that the increased ISM rainfall may be mainly driven by the enhanced moisture flux, while the dynamical processes associated with the changes in vertical motion (Fig. 4o) may tend to suppress the increase in rainfall over south-eastern zone. In addition, Table 3 documents the simulated present climate JJAS mean all-India summer monsoon rainfall (ISMR) from the selected models and B4MMM compared to OBS along with their future estimation of projected ISMR under RCP8.5 scenario. It is noted that the B4MMM well agrees with OBS in simulating present climate ISMR and its interannual standard deviation (SD). However, there are some variations among the individual selected models e.g. MPI-ESM-LR reasonably underestimates the ISMR due to dry bias over central India, but model simulates the seasonal cycle and ISV quite realistically. The future projection (2051–2099) from B4MMM compared with present climate (1951–1999) suggests increased ISMR and SD in future climate.

Fig. 5 further abstracts the contributing factors for the projected changes in rainfall over ISM domain under climate change scenario. The low level specific humidity averaged over Indian longitude (65°–95°E) shows significant increase over ISM domain due to anthropogenic global warming (Fig. 5a), thereby remarkably enhance the atmospheric instability throughout the column as evident from the change in vertically averaged equivalent potential temperature (θ_e) (Fig. 5b). This will further favour the projected increase in rainfall over ISM domain (Fig. 5c). However, the rainfall change is not sufficiently as large as the remarkable change in thermo-dynamical conditions, probably offset by the weakened vertical easterly shear over equatorial region (Fig. 5d). The projected weakening of the monsoon circulation may be related to the gradual reduction of dry static stability in both upper (Fig. 5e) and lower troposphere (Fig. 5f), thereby stabilizing the atmosphere throughout the summer season in future, which is an opposing effect of GHG-induced warming. Such changes in feedback between dynamics and moist processes in response to climate change may further modify the rainfall evolution over the ISM domain.

3.3. Future changes in interannual variability of ISM

In addition to the changes in the future mean ISM, the future estimates of year-to-year variability of ISM and the occurrence of SM/WM associated with extreme IAV are of great importance due to their potential consequences. Moreover, Sharmila et al. (2014) have recently shown that the observed seasonal mean states of SM and WM are distinctly different and could considerably modulate the ISV of ISM. Therefore, it will be worthwhile to make reliable estimates of their future changes. The IAV of ISM strength can be measured by the AIR index and different DMIs discussed in Section 2.3. Table 4 shows the correlation between AIR and three DMIs in the present climate compared to OBS and their future projections.

It is evident that B4MMM well represents the present climate relationship of AIR with WF index and MH index compared to OBS, while it underestimates the association between AIR and WY index to

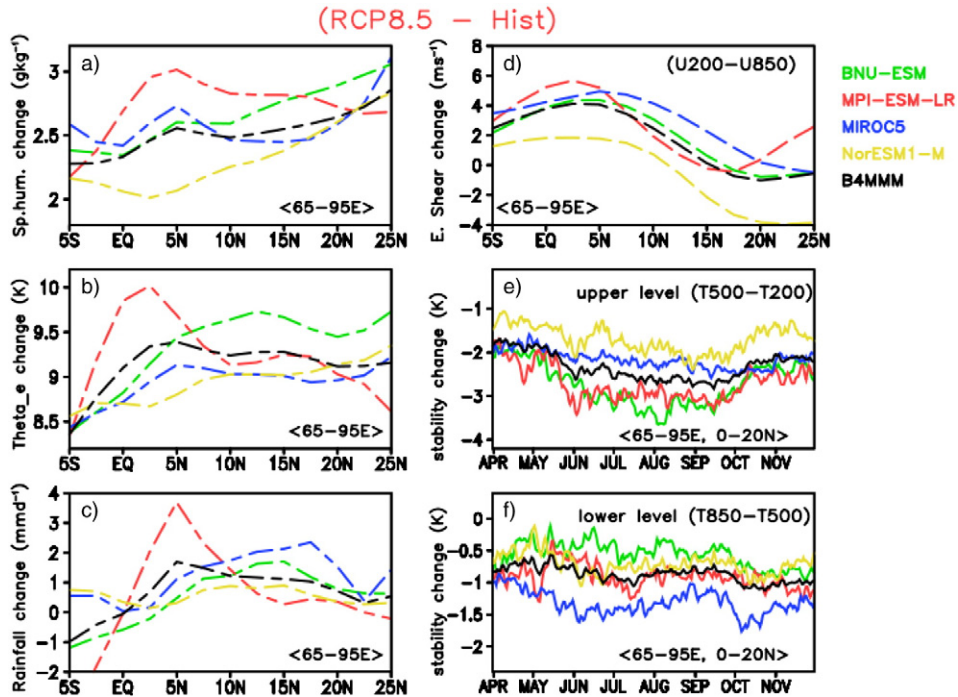


Fig. 5. Projected changes (RCP8.5 – Hist) [(2051–2099) minus (1951–1999)] in the meridional distribution of a. specific humidity at 850 hPa, b. vertically averaged equivalent potential temperature (or atmospheric instability), c. rainfall change, and d. vertical easterly shear (U_{200} – U_{850}) averaged over Indian longitude (65°–95°E). The seasonal evolution of projected changes in the atmospheric dry static stability (at upper level T_{500} – T_{200} and lower level T_{850} – T_{500}) over Indian monsoon region (65°–95°E, 0°–20°N) are also shown in e. and f. respectively for the selected models and their MMM.

Table 4

Correlation between Indian summer monsoon rainfall Index and dynamical indices and its future projection under RCP8.5 scenario.

| Experiment | Model | WY index | WF Index | MH Index |
|---|------------|--------------|-------------|-------------|
| Observed (1951–1999) | - | 0.53 | 0.78 | 0.68 |
| Historical (1951–1999) | BNU-ESM | 0.29 | 0.72 | 0.49 |
| | MPI-ESM-LR | 0.41 | 0.64 | 0.61 |
| | MIROC5 | 0.12 | 0.39 | 0.67 |
| | NorESM1-M | 0.28 | 0.80 | 0.68 |
| | B4MM | 0.28 | 0.65 | 0.61 |
| Future Projection (RCP8.5) (2051–2099) | BNU-ESM | -0.47 | 0.52 | 0.35 |
| | MPI-ESM-LR | 0.15 | 0.74 | 0.52 |
| | MIROC5 | -0.24 | 0.44 | 0.36 |
| | NorESM1-M | 0.19 | 0.55 | 0.48 |
| | B4MM | -0.09 | 0.56 | 0.43 |

some extent. It is projected that the future correlations between DMIs and AIR might be highly reduced on interannual timescale, following the future weakening of the large scale circulation associated with enhanced ISMR in a warmer climate. It appears from the results that DMIs may not be appropriate measures of future ISM strength in terms of precipitation, consistent with previous results (Kitoh et al., 1997; Dairaku and Emori, 2006). Therefore, the possible changes to IAV of ISM due to climate change are examined here using AIR index only. Then the percentages of occurrence of extreme monsoon years (i.e. SM and WM) are calculated for each simulation.

Fig. 6 further shows the relative changes to the IAV of ISM due to increased GHGs under RCP8.5 scenario. B4MM projects >30% increase (relative to present climate) in both SM and WM in future climate. Although the percentage change is variable among the models; the sign of tendency is robust. The results suggest that IAV of ISM might enhance in response to increased GHG emissions in future climate, i.e. both the SM and WM years will be more frequent.

To understand the possible spatial changes of seasonal rainfall during extreme monsoons, the composited seasonal mean precipitation during SM and WM of present climate along with future projections under RCP8.5 scenario are constructed for all the models. Fig. 7 shows the projected future changes (RCP8.5 – Hist) in seasonal mean rainfall (mm day^{-1}) during SM (left column) and WM (right column) for the selected models. The projected change indicate notable local enhancement of rainfall over monsoon core region and spatial expansion of the positive (negative) rainfall anomaly during SM (WM) over the Indian land as well as over adjoining oceanic regions. It is anticipated that the JJAS mean SM (WM) will be wetter (drier) over the core monsoon zone in the future compared to the present climate. However, the projected change in JJAS rainfall is geographically variable among the models. Previous studies found that the severe WM and SM are mostly associated with the developing phase of El-Nino Southern Oscillations (ENSO) (Pillai and Annamalai, 2012). Therefore, more occurrences of

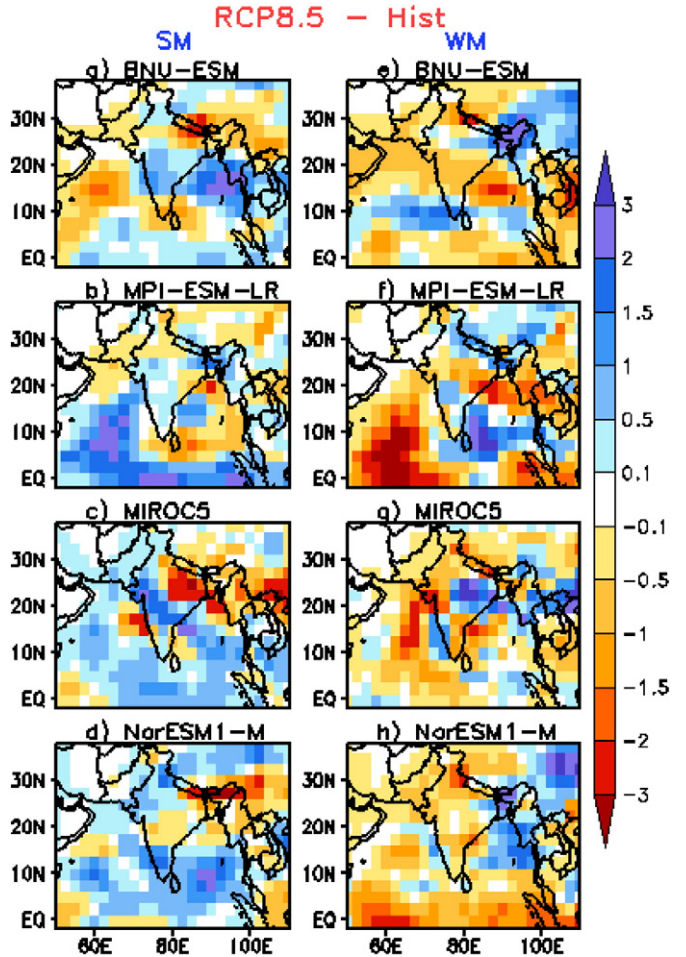


Fig. 7. Projected changes (RCP8.5 – Hist) in seasonal mean rainfall (mm day^{-1}) during strong monsoon (SM: a–d) and weak monsoon (WM: e–h) for selected models.

such extreme monsoons in future could be related to the frequency doubling of ENSO events as projected in CMIP5 (Cai et al., 2014) and which will be investigated further in a future work. The possible changes to ISV during SM and WM will be discussed in the later subsection.

3.4. Future projection of intraseasonal variability and extreme events

3.4.1. Changes in day-to-day variability

A large amount of rainfall variability is related to the occurrence of extreme rainfall events and their intensities. Any change in the individual daily rainfall events can have a large impact on JJAS mean rainfall amount (Stephenson et al., 1999). Also understanding the changes in the spatial variability of extreme rainfall events will further help to identify the projected regions of extreme variability. Therefore, in this study, the probability distribution function (PDF) of daily rainfall at each grid over ISM domain during all JJAS periods is calculated for three rain-rate categories (lighter/low: $<10 \text{ mm day}^{-1}$, moderate: $10\text{--}40 \text{ mm day}^{-1}$ and high/heavy: $>40 \text{ mm day}^{-1}$, following Mukhopadhyay et al., 2010) for all simulations.

Fig. 8 shows the projected spatial changes in the distribution of these three main rain-rate categories relative to present climate over ISM region for all models. It is noted that the projected substantial changes in the daily variability of ISM are largely associated with the increase in heavy rainfall events over Indian land and adjoining oceanic regions. Considerable decrease in the low rain-rate, even in moderate rain-rate (large change in MPI-ESM-LR) is also anticipated in future, indicating the rising climate-related vulnerability over Indian subcontinent as

Relative change (%) in Extreme Monsoon

Future climate (2051–2099) vs Present climate (1951–1999)

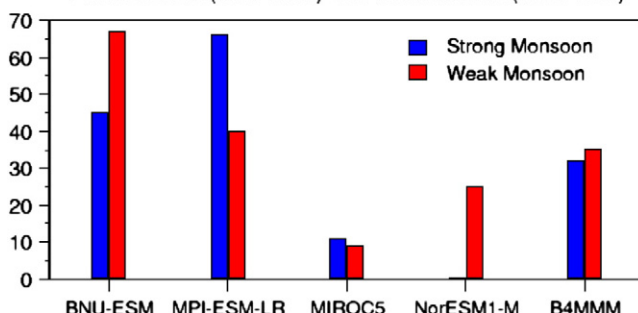


Fig. 6. Future projection of relative changes (%) in the extreme monsoon years: Strong monsoon (Blue) and Weak monsoon (Red) for selected models and their MMM.

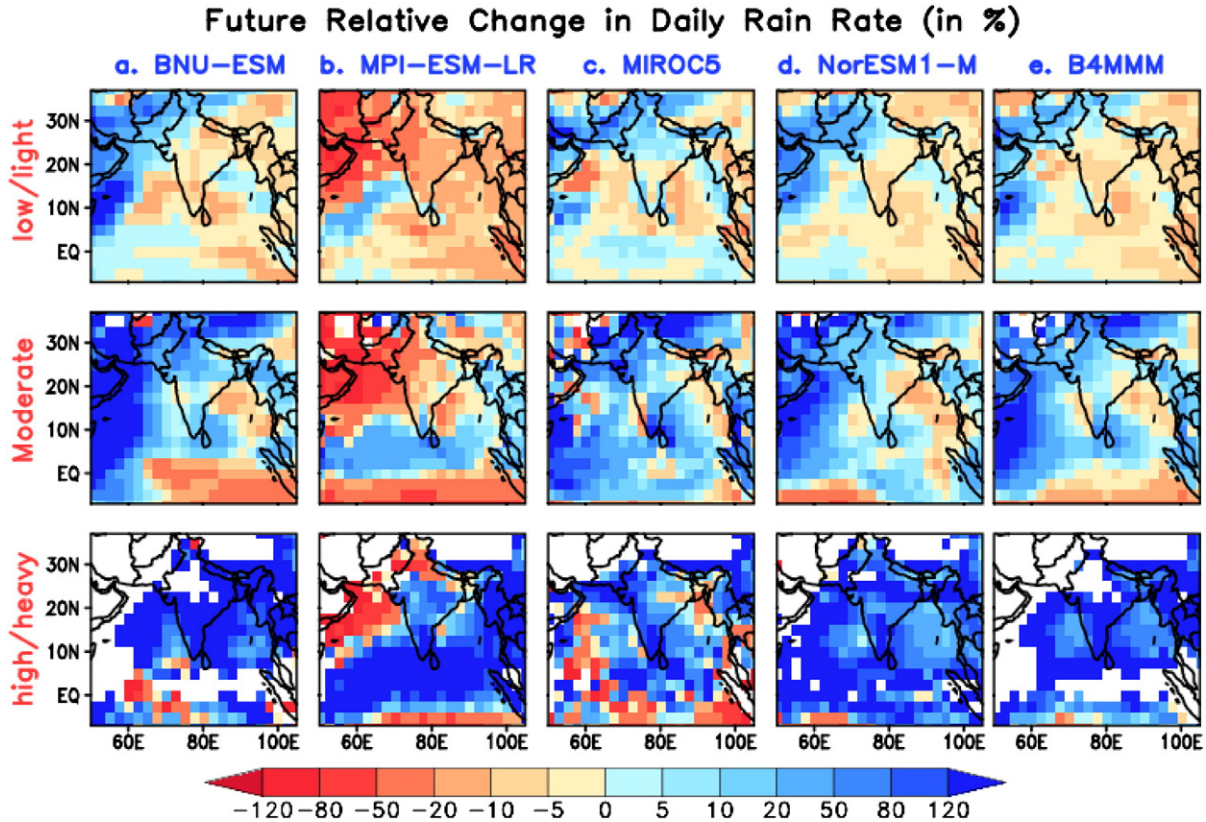


Fig. 8. Relative changes (%) in the daily rain-rate distribution (low <10 mm/day; moderate <10–40 mm/day>; and high >40 mm/day) under RCP8.5 scenario.

evident from B4MM. Such projected increase in frequency and intensity of extreme rainfall events over ISM region in the backdrop of global warming may further decrease the potential predictability of ISM variability. Together with the notable increase in extreme events in response to climate change, it is anticipated that the number of wet days may also change through the monsoon season and may affect the JJAS rainfall intensity. Here, the wet days are defined when precipitation exceeds 0.1 mm/day on a given day whereas the rainfall intensity is defined as the ratio of total seasonal precipitation divided by number of wet days per season at each grid (following Turner and Slingo, 2009).

The possible spatial changes in wet days and relative change in precipitation intensity are shown in Fig. 9. The figure illustrates that wet days over IND region might be reduced under climate change scenario; however there still exists uncertainty among the models (Fig. 9a). Most models show relatively small increase in wet days over some part of equatorial Indian Ocean but considerable decrease to the south of the equator (except MIROC5). However, the response of precipitation intensity to increased GHG forcing is large (Fig. 9b). Despite projecting a decrease in wet days, all models projected positive change in rainfall intensity over IND region particularly over western-central to peninsular Indian region, indicating the future rise in heavy rainfall events. A large north-south asymmetry in relative change in rainfall intensity is indicated over ISM region with substantial decrease over EEIO in accord with Fig. 4.

3.4.2. Possible changes in ISV activity

On the subseasonal timescale, the overall statistics of ISV activity is strongly interlaced with a large fraction of daily variability, synoptic activity and seasonal mean state of ISM. The impact of increased GHGs on future ISV remains uncertain and is one of the critical issues in monsoon climate-change research. In this subsection, we estimate the response of ISV activity in future climate from the best 4 models.

Fig. 10 shows the projected changes in the spatial distribution of intraseasonal (10–90 day bandpass filtered) variance of daily precipitation under RCP8.5 scenario. Projections suggest that future ISV will enhance over IND region, particularly over north-eastern and north-western part of Indian subcontinent. Large increase in variance is also projected over the adjoining oceanic regions; especially over EIO, Arabian Sea near Western Ghats, and head Bay of Bengal). It is noted that the projected change in the ISV activity is interlaced with the overall change in the seasonal rainfall intensity.

3.4.3. Changes to propagation characteristics

Within the 10–90 day mode of ISV activity, two dominant quasi-periodic intraseasonal timescales in the periods ranging from 10–20 days and 30–60 days cause intermittent wet/dry spells over ISM domain (Goswami, 2011). To identify the future changes in space-time characteristics of these modes, the meridional wavenumber frequency spectra of simulated daily precipitation is calculated over ISM domain (15°S – 30°N ; 65° – 95°E) during May–October from both the historical and corresponding climate change scenarios for all selected models. The model simulated spectrum of present climate shows a dominant northward propagating mode of 30–60 day period at wave-number 1 with maximum power varying at ~45–55 days in consistently from all models (figures not shown). To estimate the relative change in the dominant modes, the meridional power spectrum are averaged over 1–2 wavenumbers for all the models (Fig. 11) as the dominant 30–60 day mode of ISOs spans mostly within this range. The future change under RCP8.5 scenario shows relative enhancement (~7–10%) of power within higher frequency (15–30-day as well as below 10-day mode). While the power increases in the higher frequency modes, it substantially decreases in lower frequency (beyond 45-day) for most of the models. These results indicate a possible periodicity shift (from lower to higher frequency) of the dominant ISV modes over

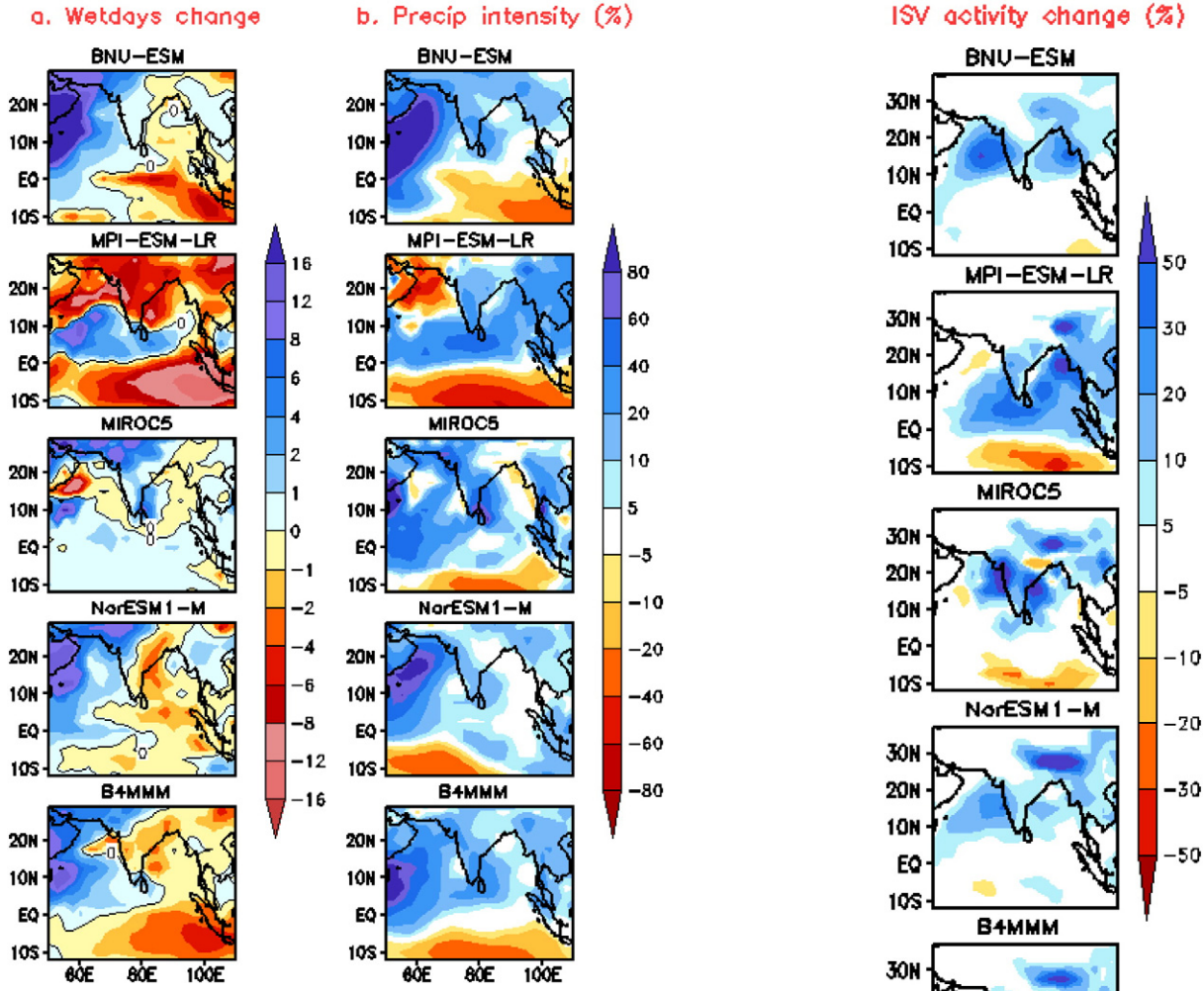


Fig. 9. a. Projected changes in the number of wet days per season of ISM and b. relative change in the summer mean rainfall intensity under RCP8.5 scenario.

ISM domain in future climate, although uncertainty still exists. It may be speculated that the increase in the high frequency ISOs may be connected with the projected extension of the westward propagating disturbances from the warmer Western Pacific into the ISM region (Fig. 4).

Now, it is worthwhile to estimate the change in the dominant northward propagating monsoon ISO under warming scenario. Fig. 12 shows the time-latitude diagrams of lag-regressed 30–70 day band-pass filtered precipitation anomalies averaged over Indian longitude (70–90°E) for present climate (*left column*) and RCP8.5 scenario (*right column*). The lag regression is performed based on first EEOF mode over ISM domain (15°S–30°N and 65°–95°E) discussed in Section 2.3. Here day 0 is considered as the day of rainfall maxima over core monsoon region. All models show prominent northward propagation of monsoon ISO from the equatorial region (around day 20) along with a realistic southward propagation in the historical simulation (Fig. 12 I). Under the increased GHGs induced climate change (Fig. 12 II), most of the models project intensified monsoon ISO around day 0 over monsoon core region. Subsequent enhanced suppression of convection over the equatorial region is also evident (largely in MPI-ESM-LR). Some models even project reduced southward propagating mode compared to present climate. It is noteworthy that the projected overall character of the dominant northward propagating low frequency monsoon ISOs (from EIO to Indian subcontinent) does not show remarkable change in a warmer climate, although the magnitude amplifies over ISM domain possibly due to moisture availability. Therefore, it may be

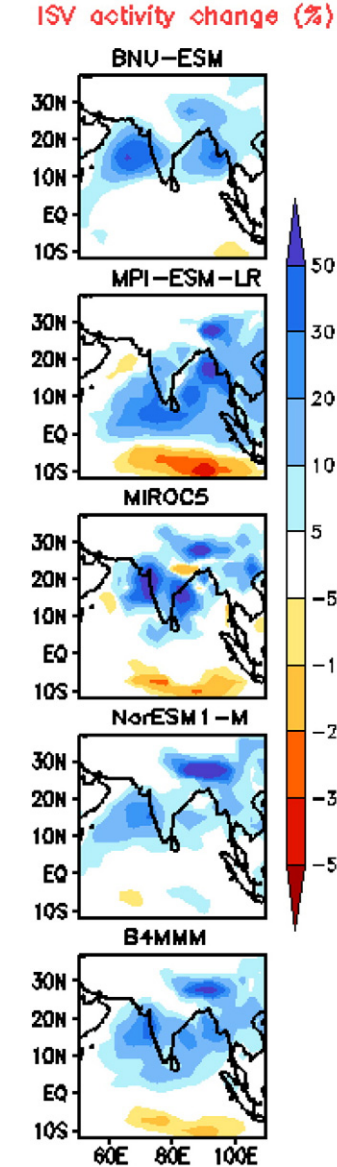


Fig. 10. Projected future relative changes (%) in the intraseasonal activity using 10–90 day band-pass filtered daily simulated rainfall under RCP8.5 scenario.

suggested that along with the amplified 30–70 day mode, the enhanced high frequency mode and periodicity shift (from high to low) of monsoon ISOs due to increased GHG induced warming may notably modulate the monsoon rainfall over Indian subcontinent in a warmer climate.

3.4.4. Future behaviour of active-break cycles

It is expected that the considerable projected increase in the higher frequency mode (below 30 day) and amplification of 30–70 day monsoon ISOs may influence the future change in the frequency and duration of these spells under enhanced GHG induced warming. To identify the possible change in the future behaviour of active-break spells, first all simulated active and break spells of the present climate and corresponding future emission scenario are identified using the method discussed in Section 2.3. The identified active/break spells are divided into two categories in terms of duration: (1) spells of 3–4 days as *short* spells, and (2) spells of duration ≥ 7 days as *long/extended* spells. The frequency distributions of simulated active/break spells from historical runs are then compared with OBS, calculated from IMD daily rainfall for the same period (1951–1999). It is noted that the frequency

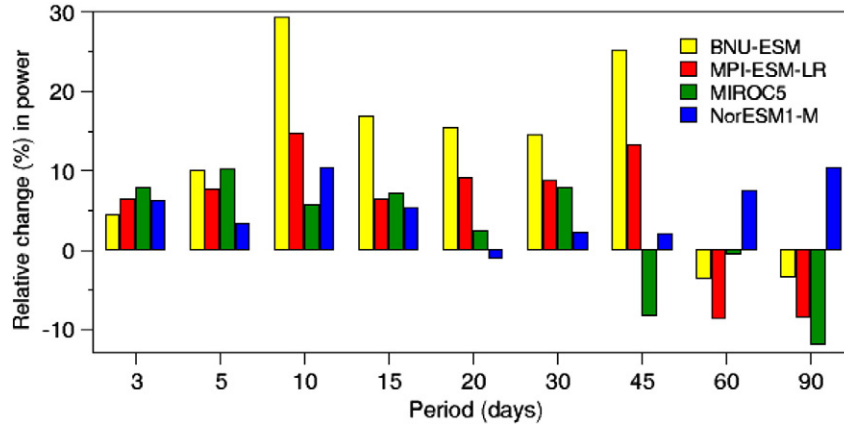


Fig. 11. Projected relative changes (%) in the meridional power spectra (northward component) of daily precipitation averaged over wavenumbers 1–2 during boreal summer over Indian domain (15°S–30°N; 60°E–95°E).

distribution (in percentage) for active/break spells simulated from historical runs of all selected models are almost comparable with OBS (Fig. 13a). This again affirms the reliability of the chosen models for studying ISV of ISM in this present study. The simulated present climate

active/breaks during extreme monsoons also capture the observed asymmetry of duration, i.e. preference of long (short) active spells during SM (WM) and extended (short) breaks during WM (SM) (Sharmila et al., 2014) to some extent (figure not shown). Now to examine the

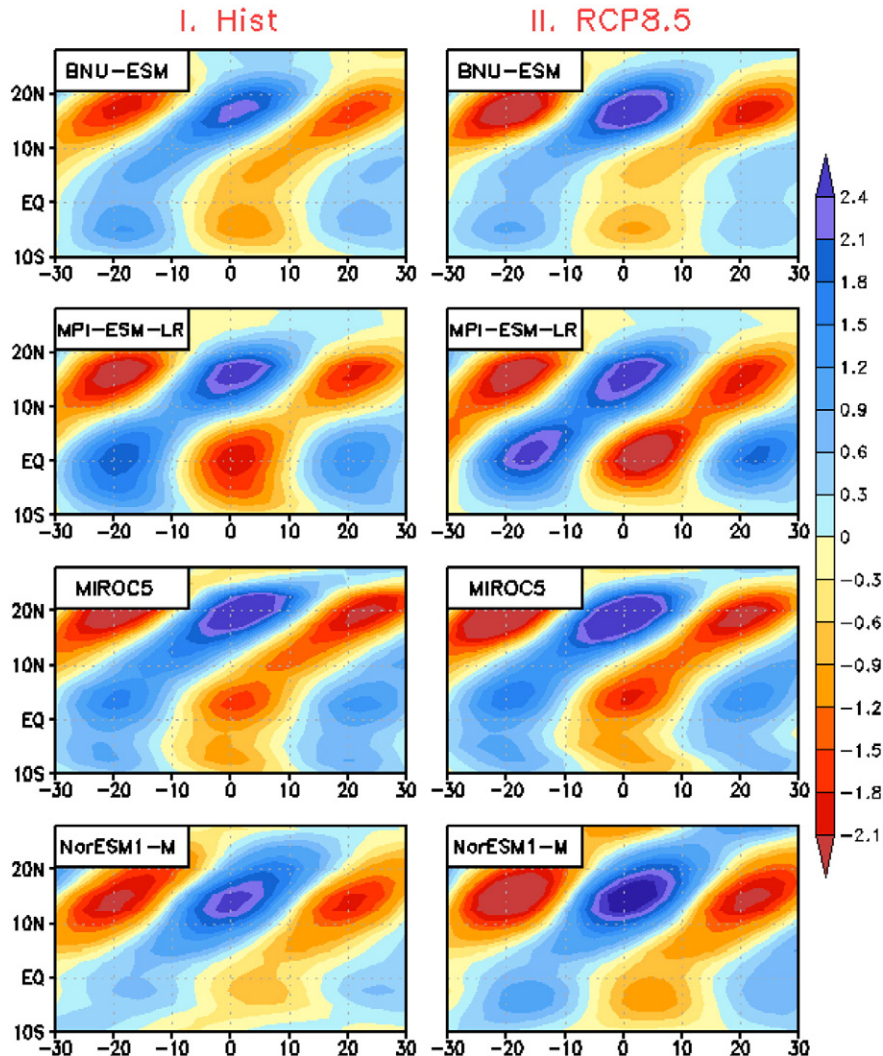


Fig. 12. Time-latitude diagram of regressed 30–70 day filtered precipitation anomalies averaged over 70°E–90°E for historical run (left column) and following RCP8.5 scenario (right column) respectively. This corresponds to first EEOF mode of intraseasonally filtered precipitation over 15°S–30°N and 65°–95°E domain during June to September.

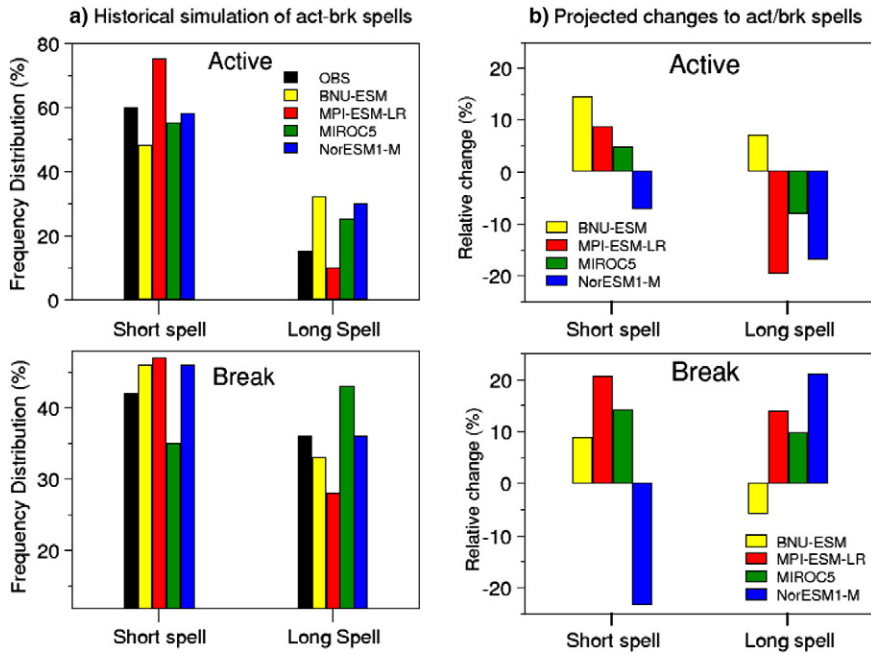


Fig. 13. a. Frequency distribution (%) of active/break spells divided into two categories in terms of duration: short (3–4 days) and long spells (≥ 7 days) in historical runs compared to observation for the period of 1951–1999, and b. Projected relative changes (%) during 2051–2099 under RCP8.5 scenario.

possible change in 21st century climate, the relative change in the spells under RCP8.5 scenario is shown in Fig. 13b. Most of the models project a relative increase of ~5–15% in short active spells, even in the spells of 5–6 days (figure not shown), while ~8–20% relative decrease in long active spells compared to present climate in response to increased GHG warming. For break spells, relative increase of 10–20% has been projected in both short and extended breaks with moderate consistency.

Moreover, the relative changes in active/break spells during extreme monsoon years are also projected. Fig. 14 shows that the longer active

spells will be more frequent, while breaks will be fewer and shorter, leading to wetter SM in future. In contrast, WM will be drier due to the high propensity of extended breaks and short active spells in response to enhanced GHG, thereby increasing the risk of both the floods and drought like conditions over Indian subcontinent in future climate.

Now, to assess the spatial changes in the active-break cycles under climate change scenario, active-break days are identified (discussed in Section 2.3) and composites of active and break phases are constructed using 10–90 day filtered precipitation anomalies. Fig. 15a–f shows the spatial composite of active spells from historical simulation compared to OBS (1st column). It illustrates that the modelled patterns of present climate large scale organized positive precipitation anomalies around the core monsoon zone, the suppressed convection over EIO and the eastward tilted structure resemble well with GPCP (Fig. 15a). The corresponding changes in active composite under RCP8.5 scenario are shown in Fig. 15g–k (2nd column). Consistent among the models, B4MM projected regionally enhanced rainfall over core monsoon zone along with dominant east-west variation over ISM domain. Moreover, enhanced suppression of rainfall over Bay of Bengal is also projected. It is speculated that the projected enhancement of high frequency mode of monsoon ISOs may enhance regional character of the future active spells. In similar manner, the simulated break composites of present climate are shown and the prime features are well captured in the historical runs for all selected models (3rd column; Fig. 15l–q). The projections show further suppression of rainfall around the core monsoon zone of Indian land during breaks under enhanced GHG-induced warming (last column; Fig. 15r–v). The robustness of these projected results across the selected models provide confidence in suggesting that the precipitation anomalies would become more intense and regionally extend over Indian land during active/break cycles in future climate. Such intensification of the active-break cycles may be caused by the overall intensification in the hydrological cycles due to significant change in the moisture content along with the substantial changes in the large scale circulation.

Similarly, the projected spatial changes in the precipitation anomalies during active/break phases of SM and WM are shown in Fig. 16. The projected change in active composite during SM shows enhanced precipitation over core monsoon region (Fig. 16 la–d) in future, while

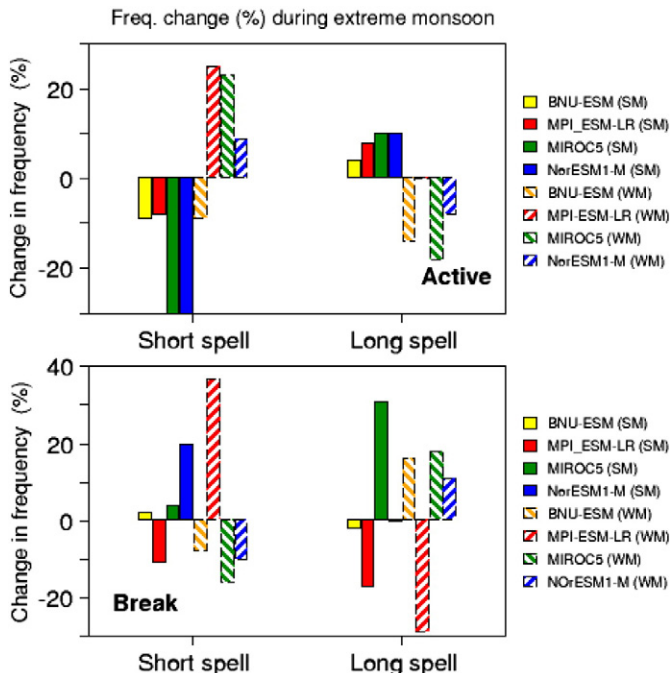


Fig. 14. Projected changes (%) in the frequency of active-break spells during strong monsoon (solid lined bar) and weak monsoon (dash lined bar) under climate change scenario.

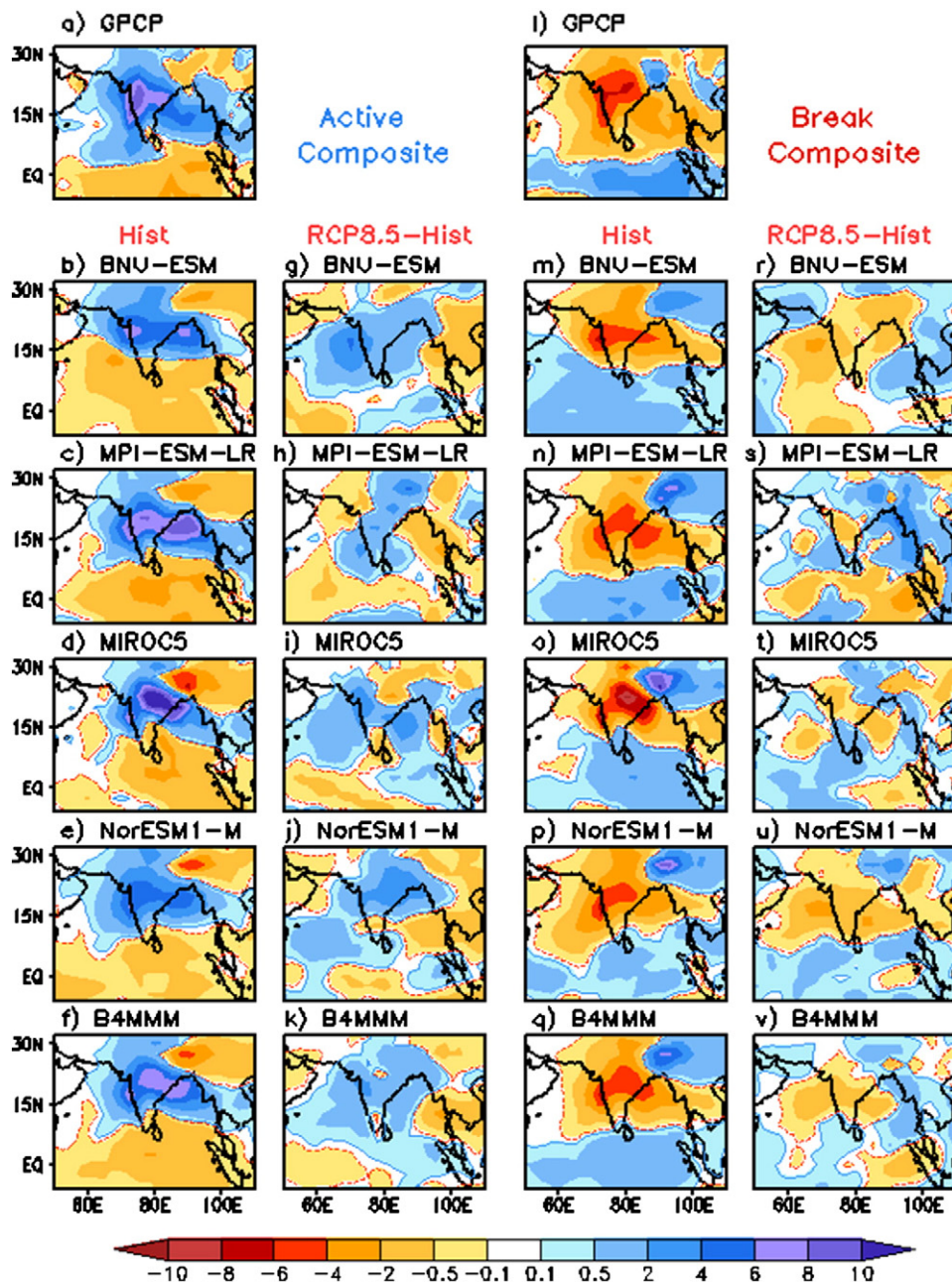


Fig. 15. Active composite of 10–90 day filtered daily precipitation anomalies as simulated in the historical runs (a–f; 1st column) compared to OBS (GPCP) and corresponding change under RCP8.5 scenario (g–k; 2nd column). Similarly break composites are shown in l–v for selected models and their MMM.

reduced rainfall is evident during active phase of WM (Fig. 16 le-h) in most of the models (except MIROC5). Such changes are probably linked with the projected increase in the frequency of longer (shorter) active spells during SM (WM) in future as discussed earlier. Consistent results are also noted in projecting future spatial changes in break composites. Fig. 16.II shows that the breaks might be weaker (stronger) during SM (WM), over core monsoon zone during WM consistent with Fig. 14. Therefore, it could be summarised that the present climate ISV during extreme monsoon will be more severe and intense in future climate. However, the projected changes are variable geographically and therefore uncertain among the selected models.

4. Concluding remarks

The endurance of the growing populations and the developing socio-economic situations in India are predominantly interlaced with

ISM variability. Thus, any change in monsoon rainfall due to enhanced GHG-induced climate change will have undeviating implications on water resources, agricultural output, public health and economy of the subcontinent. In this study, the potential future spatio-temporal changes in different aspects of ISM variability have been assessed using 20 state-of-the-art climate models from CMIP5 under RCP8.5 climate change scenario. Optimal selection criteria have been used to identify most realistic and reliable climate models in simulating the basic features of ISM variability. Out of twenty models, only four models (viz. BNU-ESM, MPI-ESM-LR, MIROC5 and NorESM1-M) are able to reproduce some of the salient features of the ISM realistically. These models are then selected for further climate change analysis. The model results show that the response to climate change is plausibly consistent among the selected models, especially among the ESMs. Under the climate change scenario, the robustness of the projected results across the four better models and B4MMM provides confidence to suggest that

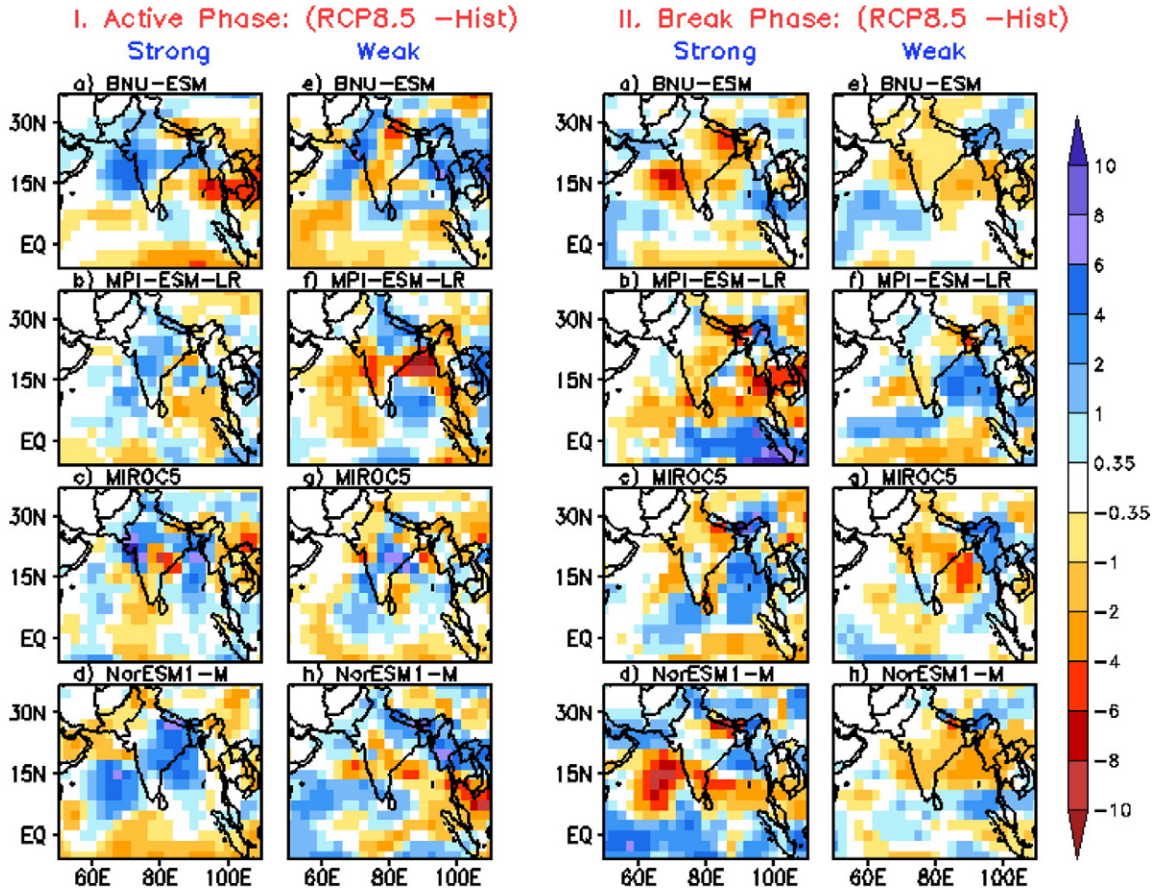


Fig. 16. Projected changes (RCP8.5 –Hist) [(2051–2099) minus (1951–1999)] in the composited active (I.) and break (II.) phases using 10–90 day filtered daily precipitation anomalies during strong (I. a–d and II. a–d) and weak monsoon (I. e–h and II. e–h) years respectively.

the overall future change in ISM rainfall is accompanied by the substantial changes in the variability on different time scales, ranging from daily to subseasonal to interannual variations during boreal summer beyond the mid 21st century.

On seasonal-to-interannual timescales, the model projections indicate that the seasonal mean ISMR and its IAV may noticeably increase in future climate. It may primarily be driven by the considerable increase in the thermodynamic conditions over ISM region due to GHG-induced warming, although slightly offset by weakening of the large scale monsoon circulation and the stabilization of atmosphere in warmer climate. It is expected that the rainfall magnitude might amplify over the core monsoon zone and length of the season may enhance due to late withdrawal, with no change in monsoon onset time. Further, model projections on IAV of ISM suggest that severity and frequency of both the SM and WM seasons may increase in future climate. However, projected change in the spatial patterns of seasonal rainfall during extreme monsoon is variable at regional scales with some uncertainty.

The PDF analysis of daily precipitation at each grid indicates that there could be significant enhancement in heavy rainfall events (>40 mm/day) over ISM domain along with reduced low rain-rate (<10 mm/day) events and decrease in number of wet days. However an increase in seasonal mean rainfall intensity is anticipated in future climate. On subseasonal scale, considerable changes in spatio-temporal scales of the ISV have been projected among the models with notable enhancement of 10–90 day ISV activity over Indian Ocean to the north of the equator. The meridional wavenumber frequency spectra of future daily precipitation over ISM domain indicate considerable amplification of higher frequency components of monsoon ISOs during boreal summer in response to enhanced GHG warming. However, the projected overall character of the dominant northward

propagating 30–70 day mode monsoon ISOs does not show remarkable change in a warmer climate, although the magnitude amplifies over ISM domain possibly due to moisture availability. The models further project that the future active/break cycles might be more intense and regionally extended in future climate, with enhanced propensity of both short and long active/break spells. Moreover, the projection of ISV during extreme monsoon also indicate that SM might be wetter in future due to increase in persistent active spells with decreasing break spells, whereas WM would be drier with possible increase in very long breaks and shorter actives in future. These results indicate more severe drought and flood like conditions over Indian subcontinent in future climate. However, the projected changes in spatial structure of active/break during extreme monsoon years are geographically variable among the selected models.

It is worth to be noted that a small amount of uncertainty in projecting various aspects of ISM variability still exists among the selected models; e.g. the uncertainty in projecting ISV during extreme monsoons could be attributed to significant underestimations of ISMR-ENSO teleconnection and other physical processes by CMIP5 models (Jourdain et al., 2013). However, assessing the role of such changes is beyond the scope of this study. The internal variability of the climate models could also introduce some uncertainty in the model projection (Deser et al., 2012), which has been ignored in this study by considering only one ensemble of each model. The nature of such projections of ISM variability however, could also be complicated by the uncertain role of aerosols. The direct/indirect radiative effects of atmospheric aerosol loading represented in these CMIP5 models could add more uncertainty in the future estimation as they are considered to influence the present-climate monsoon variability in various ways (Ballasina et al., 2011; Manoj et al., 2011). Nevertheless, the consistent projections from the

selected models in most of the aspects of ISM variability offer more confidence in the results and suggest the requisite of profound adaptation measures and better policy making in future.

Acknowledgements

This research work is a part of the Ph.D. thesis of S.S. financially supported by the Council for Science and Industrial Research (CSIR) New Delhi, India. The authors thanks Prof. B. N. Goswami, former Director IITM for his encouragement and support to carry out this research work. The authors wish to acknowledge the Editor Dr. K. McGuffie, and the two anonymous reviewers for their insightful comments and suggestions that helped to improve the earlier manuscript. World Climate Research Programme's Working Group on Coupled Modelling, which is responsible for CMIP, along with the climate modelling groups (listed in Table 1) are duly acknowledged. For CMIP the U.S. Department of Energy's Program for Climate Model Diagnosis and Intercomparison provides coordinating support and led development of software infrastructure in partnership with the Global Organization for Earth System Science Portals. S.S. also thanks S.P. Gharde for his assistance in data download and Abhik S. for useful discussions. The figures are prepared using GrADS and XMGRACE. IITM is fully supported by the Ministry of Earth Sciences, Govt. of India.

References

- Annamalai, H., 2011. Modelling the monsoons in a changing climate. In: Carayannis, Elias (Ed.), *Planet Earth 2011 – Global warming challenges and opportunities for policy and practice*. ISBN: 978-953-307-733-8.
- Annamalai, H., Hafner, J., Sooraj, K.P., Pillai, P., 2013. Global warming shifts the monsoon circulation, drying South Asia. *J. Clim.* 26, 2701–2718. <http://dx.doi.org/10.1175/JCLI-D-12-00208.1>.
- Ashfaq, M., Shi, Y., Tung, W., et al., 2009. Suppression of south Asian summer monsoon precipitation in the 21st century. *Geophys. Res. Lett.* 36, L01704. <http://dx.doi.org/10.1029/2008GL036500>.
- Bhaskaran, B., Mitchell, J.F.B., Lavery, J.R., Lal, M., 1995. Climatic response of the Indian subcontinent to doubled CO₂ concentrations. *Int. J. Climatol.* 15, 873–892. <http://dx.doi.org/10.1002/joc.3370150804>.
- Bollasina, M.A., Ming, M., Ramaswamy, V., 2011. Anthropogenic aerosols and the weakening of the South Asian summer monsoon. *Science* 334, 502–505.
- Cai, W., Borlace, S., Lengaigne, et al., 2014. Increasing frequency of extreme El Niño events due to greenhouse warming. *Nat. Clim. Chang.* <http://dx.doi.org/10.1038/NCLIMATE2100>.
- Cherchi, A., Alessandri, A., Masina, S., Navarra, A., 2011. Effects of increased CO₂ levels on monsoon. *Clim. Dyn.* 37, 83–101. <http://dx.doi.org/10.1007/s00382-010-0801-7>.
- Dairaku, K., Emori, S., 2006. Dynamic and thermodynamic influences on intensified daily rainfall during the Asian summer monsoon under doubled atmospheric CO₂ conditions. *Geophys. Res. Lett.* 33, L01704. <http://dx.doi.org/10.1029/2005GL024754>.
- Dash, S.K., Kulkarni, M.A., Mohanty, U.C., Prasad, K., 2009. Changes in the characteristics of rain events in India. *J. Geophys. Res.* 114, D10109. <http://dx.doi.org/10.1029/2008JD010572>.
- Deser, C., Phillip, A., Bourdette, V., Teng, H., 2012. Uncertainty in climate change projections: the role of internal variability. *Clim. Dyn.* 38, 527–546. <http://dx.doi.org/10.1007/s00382-010-0977-x>.
- Duchon, C.E., 1979. Lanczos filtering in one and two dimensions. *J. Appl. Meteorol.* 18, 1016–1022.
- Gadgil, S., Rupa Kumar, K., 2006. The Asian monsoon-agriculture and economy. In: Wang, B. (Ed.), *The Asian monsoon*. Springer, Berlin, pp. 651–683.
- Ghosh, S., Das, D., Kao, S.C., Ganguly, A.R., 2012. Lack of uniform trends but increasing spatial variability in observed Indian rainfall extremes. *Nat. Clim. Chang.* 2, 86–91. <http://dx.doi.org/10.1038/NCLIMATE1327>.
- Goswami, B.N., 2011. South Asian summer monsoon. In: Lau, W.K.-M., Waliser, D.E. (Eds.), *Intraseasonal variability of the atmosphere-ocean climate system*, 2nd edn Springer, Berlin, pp. 21–72.
- Goswami, B.N., Krishnamurthy, V., Annamalai, H., 1999. A broad-scale circulation index for the interannual variability of the Indian summer monsoon. *Q. J. R. Meteorol. Soc.* 125, 611–633. <http://dx.doi.org/10.1002/qj.49712555412>.
- Goswami, B.N., Venugopal, V., Sengupta, D., et al., 2006. Increasing trend of extreme rain events over India in a warming environment. *Science* 314 (80), 1442–1445.
- Guhathakurta, P., Rajeevan, M., 2008. Trends in the rainfall pattern over India. *Int. J. Climatol.* 28, 1453–1469. <http://dx.doi.org/10.1002/joc>.
- Held, I.M., Soden, B.J., 2006. Robust responses of the hydrological cycle to global warming. *J. Clim.* 19, 5686–5699.
- Hsu, P.C., Li, T., Luo, J.J., Murakami, H., Kitoh, A., Zhao, M., 2012. Increase of global monsoon area and precipitation under global warming: a robust signal? *Geophys. Res. Lett.* 39, L0670. <http://dx.doi.org/10.1029/2012GL051037>.
- Hsu, P., Li, T., Murakami, H., Kitoh, A., 2013. Future change of the global monsoon revealed from 19 CMIP5 models. *J. Geophys. Res.: Atmos.* 118, 1–14. <http://dx.doi.org/10.1002/jgrd.50145>.
- Hu, Z., Latif, M., E.R., Bengtsson, L., 2000. Intensified Asian summer monsoon and its variability in a coupled model forced by increasing greenhouse gas concentrations. *Geophys. Res. Lett.* 27, 2681–2684.
- Huffman, G.J., Adler, R.F., Bolvin, D.T., Gu, G., 2009. Improving the global precipitation record: GPCC version 2.1. *Geophys. Res. Lett.* 36, L17808. <http://dx.doi.org/10.1029/2009GL040000>.
- IPCC, 2007. *Climate change 2007 – The physical science basis contribution of working group I to the fourth assessment report of the IPCC* (ISBN 978 0521 88009-1 Hardback; 0521 70596-7 paperback).
- Joseph, S., Sahai, A.K., Goswami, B.N., Terray, P., Masson, S., Luo, J.J., 2012. Possible role of warm SST bias in the simulation of boreal summer monsoon in SINTEX-F2 coupled model. *Clim. Dyn.* 38, 1561–1576. <http://dx.doi.org/10.1007/s00382-011-1264-1>.
- Jourdain, N.C., Sen Gupta, A., Taschetto, et al., 2013. The Indo-Australian monsoon and its relationship to ENSO and IOD in reanalysis data and the CMIP3/CMIP5 simulations. *Clim. Dyn.* 41 (11–12), 3073–3102. <http://dx.doi.org/10.1007/s00382-013-1676-1>.
- Kalnay, E., et al., 1996. The NCEP/NCAR 40-year reanalysis project. *Bull. Am. Meteorol. Soc.* 77, 437–471.
- Kitoh, A., Yukimoto, S., Noda, A., Motoi, T., 1997. Simulated changes in the Asian summer monsoon at times of increased atmospheric CO₂. *J. Meteorol. Soc. Jpn.* 75 (6), 1019–1031.
- Kitoh, A., Endo, H., Krishna Kumar, K., et al., 2013. Monsoons in a changing world: A regional perspective in a global context. *J. Geophys. Res. Atmos.* 118, 3053–3065. <http://dx.doi.org/10.1002/jgrd.50258>.
- Kripalani, R.H., Kulkarni, A., Sabade, S.S., 2003. *Indian monsoon variability in a global warming scenario*. *Nat. Hazards* 29, 189–206.
- Kripalani, R.H., Oh, J.H., Kulkarni, A., Sabade, S.S., Chaudhari, H.S., 2007. *South Asian summer monsoon precipitation variability: coupled climate model simulations and projections under IPCC AR4*. *Theor. Appl. Climatol.* 90, 133–159.
- Krishna Kumar, K., Patwardhan, S.K., Kulkarni, A., Kamala, K., Rao, K.K., Jones, R., 2011. Simulated projections for summer monsoon climate over India by a high-resolution regional climate model (PRECIS). *Curr. Sci. (ISSN: 0011-3891)* 101 (3), 312–326.
- Krishnan, R., Sabin, T.P., Ayantika, D.C., et al., 2013. Will the South Asian monsoon overturning circulation stabilize any further? *Clim. Dyn.* 40, 187–211.
- Lal, M., Nozawa, T., Emori, S., et al., 2001. Future climate change: Implications for Indian summer monsoon and its variability. *Curr. Sci.* 81, 1196–1207.
- Lau, W.K.M., Wu, H.T., Kim, K.M., 2013. A canonical response of precipitation characteristics to global warming from CMIP5 models. *Geophys. Res. Lett.* 40, 3163–3169. <http://dx.doi.org/10.1002/grl.50420>.
- Lee, J.-Y., Wang, B., 2014. Future change of global monsoons in the CMIP5. *Clim. Dyn.* 42, 101–119. <http://dx.doi.org/10.1007/s00382-012-1564-0>.
- Mandekar, S.K., Sahai, A.K., Shinde, M.A., Joseph, S., Chattopadhyay, R., 2007. Simulated changes in active/break spells during the Indian summer monsoon due to enhanced CO₂ concentrations: assessment from selected coupled atmosphere–ocean global climate models. *Int. J. Climatol.* 27, 837–859.
- Manoj, M.G., Devara, P.C.S., Safai, P.D., Goswami, B.N., 2011. Absorbing aerosols facilitate transition of Indian monsoon breaks to active spells. *Clim. Dyn.* 37, 2181–2198. <http://dx.doi.org/10.1007/s00382-010-0971-3>.
- May, W., 2004. Variability and extremes of daily rainfall during the Indian summer monsoon in the period 1901–1989. *Glob. Planet. Chang.* 44, 83–105. <http://dx.doi.org/10.1016/j.gloplacha.2004.06.007>.
- May, W., 2011. The sensitivity of the Indian summer monsoon to a global warming of 2°C with respect to pre-industrial times. *Clim. Dyn.* 37 (9), 1843–1868.
- Meehl, G.A., Washington, W.M., 1993. South Asian summer monsoon variability in a model with doubled atmospheric carbon dioxide concentration. *Science* 260 (5111), 1101–1104. <http://dx.doi.org/10.1126/science.260.5111.1101>.
- Meehl, G.A., Covey, C., Delworth, T., Latif, M., et al., 2007. The WCRP CMIP3 multi-model dataset: a new era in climate change research. *Bull. Am. Meteorol. Soc.* 88, 1383–1394.
- Mukhopadhyay, P., Taraphdar, S., Goswami, B.N., Krishna Kumar, K., 2010. Indian summer monsoon precipitation climatology in a high resolution regional climate model: Impact of convective parameterization on systematic biases. *Weather Forecast.* 25, 369–387. <http://dx.doi.org/10.1175/2009WAF2223201>.
- Pillai, P.A., Annamalai, H., 2012. Moist dynamics of severe monsoons over south Asia: Role of the tropical SST. *J. Atmos. Sci.* 69, 97–115. <http://dx.doi.org/10.1175/JAS-D-11-056.1>.
- Rajeevan, M., Pai, D.S., Kumar, A.R., Lal, B., 2006. New statistical models for long-range forecasting of southwest monsoon rainfall over India. *Clim. Dyn.* 28, 813–828. <http://dx.doi.org/10.1007/s00382-006-0197-6>.
- Rajeevan, M., Bhate, J., Jaswal, A.K., 2008. Analysis of variability and trends of extreme rainfall events over India using 104 years of gridded daily rainfall data. *Geophys. Res. Lett.* 35, L1870. <http://dx.doi.org/10.1029/2008GL035143>.
- Rajeevan, M., Gadgil, S., Bhate, J., 2010. Active and break spells of the Indian summer monsoon. *J. Earth Syst. Sci.* 119, 229–247.
- Rupa Kumar, K., Sahai, A.K., Kumar, K.K., Patwardhan, S.K., Mishra, P.K., Revadekar, J.V., Kamala, K., Pant, G.B., 2006. High resolution climate changes scenarios for India for the 21st century. *Curr. Sci.* 90, 334–345.
- Sabeerali, C.T., Dandi, A.R., Dhakate, A., Salunke, K., Mahapatra, S., Rao, S.A., 2013. Simulation of boreal summer intraseasonal oscillations in the latest CMIP5 coupled GCMs. *J. Geophys. Res.* 118, 4401–4420. <http://dx.doi.org/10.1002/jgrd.50403>.
- Sharmila, S., Joseph, S., Chattopadhyay, R., Sahai, A.K., Goswami, B.N., 2014. Asymmetry in space-time characteristics of Indian summer monsoon intraseasonal oscillations during extreme years – Role of seasonal mean state. *Int. J. Climatol.* <http://dx.doi.org/10.1002/joc.4100>.
- Singh, D., Tsang, M., Rajaratnam, B., Diffenbaugh, N.S., 2014. Observed changes in extreme wet and dry spells during the South Asian summer monsoon season. *Nat. Clim. Chang.* <http://dx.doi.org/10.1038/NCLIMATE2208>.

- Sperber, K.R., Annamalai, H., Kang, I.-S., et al., 2012. The Asian summer monsoon: an inter-comparison of CMIP5 vs. CMIP3 simulations of the late 20th century. *Clim. Dyn.* 41, 2711–2744. <http://dx.doi.org/10.1007/s00382-012-1607-6>.
- Stephenson, D.B., Rupa Kumar, K., Doblas-Reyes, F.J., Royer, J.F., Chauvin, F., Pezzulli, S., 1999. Extreme daily rainfall events and their impact on ensemble forecasts of the Indian monsoon. *Mon. Weather Rev.* 127, 1954–1966.
- Stowasser, M., Annamalai, H., Hafner, J., 2009. Response of the south Asian summer monsoon to global warming: Mean and synoptic systems. *J. Clim.* 22, 1014–1036.
- Tanaka, H.L., Ishizaki, N., Nohara, D., 2005. Intercomparison of the intensities and trends of Hadley, Walker, and Monsoon circulations in the global warming projects. *SOLA* 1, 077–080.
- Taylor, K.E., 2001. Summarizing multiple aspects of model performance in a single diagram. *J. Geophys. Res.* 106 (D7), 7183–7192.
- Taylor, K.E., Stouffer, R.J., Meehl, G.A., 2012. An overview of CMIP5 and the experiment design. *Bull. Am. Meteorol. Soc.* 93, 485–498. <http://dx.doi.org/10.1175/BAMS-D-11-00094.1>.
- Turner, A.G., 2011. Modelling monsoons: Understanding and predicting current and future behaviour. In: Chang, C., Ding, Y., Lau, N., et al. (Eds.), *Glob. Monsoon Syst. Res. Forecast*, 2nd edition World Scientific; WMO, pp. 421–454.
- Turner, A.G., Annamalai, H., 2012. Climate change and the south Asian summer monsoon. *Nat. Clim. Chang.* 2, 587–595.
- Turner, A.G., Slingo, J.M., 2009. Subseasonal extremes of precipitation and active-break cycles of the Indian summer monsoon in a climate-change scenario. *Q. J. R. Meteorol. Soc.* 135, 549–567. <http://dx.doi.org/10.1002/qj>.
- Turner, A.G., Inness, P.M., Slingo, J.M., 2007. The effect of doubled CO₂ and model basic state biases on the monsoon-ENSO system. I: Mean response and interannual variability. *Q. J. R. Meteorol. Soc.* 133, 1143–1157. <http://dx.doi.org/10.1002/qj>.
- Ueda, H., Iwai, A., Kuwako, K., Hori, M.E., 2006. Impact of anthropogenic forcing on the Asian summer monsoon as simulated by eight GCMs. *Geophys. Res. Lett.* 33, L06703. <http://dx.doi.org/10.1029/2005GL025336>.
- Wang, B., Fan, Z., 1999. Choice of south Asian summer monsoon indices. *Bull. Am. Meteorol. Soc.* 80, 629–638.
- Wang, B., Yim, S.-Y., Lee, J.-Y., Liu, J., Ha, K.-J., 2014. Future change of Asian-Australian monsoon under RCP 4.5 anthropogenic warming scenario. *Clim. Dyn.* 42, 83–100. <http://dx.doi.org/10.1007/s00382-013-1769-x>.
- Webster, P.J., Yang, S., 1992. Monsoon and ENSO: Selectively interactive systems. *Q. J. R. Meteorol. Soc.* 118, 877–926. <http://dx.doi.org/10.1002/qj.49711850705>.
- Wheeler, M., Kiladis, G.M., 1999. Convectively coupled equatorial waves: Analysis of clouds and temperature in the wavenumber-frequency domain. *J. Atmos. Sci.* 56, 374–399.